Materials Advances

ROYAL SOCIETY OF CHEMISTRY

REVIEW

View Article Online
View Journal | View Issue

Cite this: *Mater. Adv.*, 2022, 3, 5186

Carbon-based electrically conductive materials for bone repair and regeneration

Rebeca Arambula-Maldonado [a] and Kibret Mequanint *[ab]

Electrically conductive polymers and carbon-based materials are emerging as promising biomaterials for applications in bone tissue engineering solutions. Carbon-based conductive materials may be more suitable alternatives due to their ability to adsorb proteins, act as load-bearing materials, and accelerate bone regeneration and maturation through exogenous electrical stimulation. Furthermore, incorporating carbon-based conductive materials into bone tissue engineering scaffolds better mimics the natural structural and electrically conductive properties of the native bone. This review discusses the *in vitro* and *in vivo* performances of one-dimensional and two-dimensional carbon-based conductive materials and their applications as three-dimensional scaffolds for bone tissue engineering. Cellular processing mechanisms of carbon-based conductive materials are summarized to understand better the cellular uptake, degradation, and excretion of these conductive materials if they were to be delivered to the human body to treat bone defects. Both *in vitro* and *in vivo* models are discussed to provide insight into the role played by the carbon-based electrically conductive bone scaffold, which may lead to clinical translation.

Received 5th January 2022,
Accepted 10th May 2022

DOI: 10.1039/d2ma00001f

rsc.li/materials-advances

[a] *School of Biomedical Engineering, University of Western Ontario, 1151 Richmond Street, London, N6A 5B9, Canada. E-mail: kmequani@uwo.ca; Fax: +1-(519) 661-3498; Tel: +1-(519) 661-2111 ext. 88573*

[b] *Department of Chemical and Biochemical Engineering, University of Western Ontario, 1151 Richmond Street, London, N6A 5B9, Canada*

1. Introduction

By 2025 there will be over 3 million cases of bone fractures in the United States that require clinical intervention, creating an increased medical system cost of $25 billion per year.[1] In

Rebeca Arambula-Maldonado

Rebeca completed her undergraduate degree in Biotechnology Engineering at Instituto Tecnológico y de Estudios Superiores de Monterrey (ITESM) in Monterrey, Mexico, from 2010 to 2015. In 2016, she moved to The University of Sheffield, UK, to study her MSc degree in Stem Cells and Regenerative Medicine, during which her research focused on the molecular mechanisms by which fibroblast migration is directed during wound healing. Combining her interest in the use of biomaterials and cellular therapeutics, Rebeca joined the laboratory of Dr Kibret Mequanint at the University of Western Ontario, Canada, as a PhD candidate in 2019. Her current research is focused on the development of novel electrically conductive and bioactive scaffolds for bone repair and regeneration.

Kibret Mequanint

Kibret Mequanint is a professor in the Department of Chemical and Biochemical Engineering and the School of Biomedical Engineering at the University of Western Ontario, Canada. His research interests are biomaterials, tissue engineering, and regenerative medicine. He has published over 130 research articles in leading journals and delivered more than 65 invited talks at major international conferences and research institutions. He embodies the growing influence of biomaterials scientists and chemical engineers in life sciences and made significant contributions to degradable biomaterials design and the applications of principles of polymeric materials and chemical engineering to tissue engineering and regenerative medicine. His contributions to regenerative medicine research and education have been recognized by several national and international awards.

Canada, the healthcare system already faces an overall yearly cost of $2.3 billion for the treatment of osteoporosis and osteoporosis-related fractures,[2,3] and as the aging segment of the population increases, an ever-increasing financial burden will be imposed on the healthcare system. Repair of bone fractures and reconstruction of critical-size bone defects that exceed the natural healing ability of the human body thus represent a significant challenge.[4]

Bone defects are caused by either external factors or deformation of existing bone, resulting in structural deterioration.[5] Current intervention strategies to treat bone defects involve the replacement of the damaged region with donor bone either from autograft, allograft, or xenogeneic sources. However, the use of donor bone sources possesses significant risks, including donor-site morbidity, hemorrhaging, and an elevated risk of disease transmission.[6] Of greater concern is their limited availability, with autografts already in short supply and therefore unable to meet the increasing demand for our aging population. For these reasons, synthetic bone graft substitutes have received significant attention.

Synthetic materials were first prepared as bone graft substitutes with the design purpose to match the physical properties present in natural bone, with a minimal adverse response to the host.[7] Sustained research in this field developed biomaterials that could create a favorable interface between the implanted material and the host tissue, promoting positive responses in the surrounding tissues within the body.[8] One of the most studied bone biomaterials is bioactive glass (BG), originally 45S5 BG invented by Hench,[9] which has gained great attention due to its ability to bond to bone through the formation of hydroxyapatite layers on its surface within a physiological environment. However, the processing of synthetic bone graft substitutes into porous complex scaffolds for load-bearing implantation sites can become challenging due to their brittle and stiff nature. In addition, patients treated with scaffolds made entirely of BG displayed limited anatomical and functional recovery demonstrating the requirement for an alternative intervention solution.[10] The new solution would integrate natural or synthetic polymers to create a hybrid tissue-engineered bone that would ideally degrade at a similar rate to the formation of new tissue to maintain the integrity of the repaired region of bone which can physiologically and mechanically adapt to the natural environment and local load within the body.[11]

Although several materials such as organic polymers, inorganic phosphates, and organic–inorganic hybrids have been extensively studied for bone repair and regeneration,[12–15] new generation biomaterials that provide additional functionality for bone scaffolds such as conductivity,[16–18] fluorescence property, and drug delivery[19] are active areas of research being applied for bone tissue engineering solutions. The native bone possesses endogenous conductive properties[20,21] and the incorporation of a conductive element into a bone biomaterial could better mimic the bone's natural electrical conductivity providing significant advantages at a physiological level.[22] Carbon-based conductive materials have specifically been incorporated into polymer-based bone biomaterials as a reinforcement element and also as a component that can deliver electrical cues through the application of electrical stimulation for the maturation of osteoblasts and promotion of the repair and regeneration of bone defects (Fig. 1).

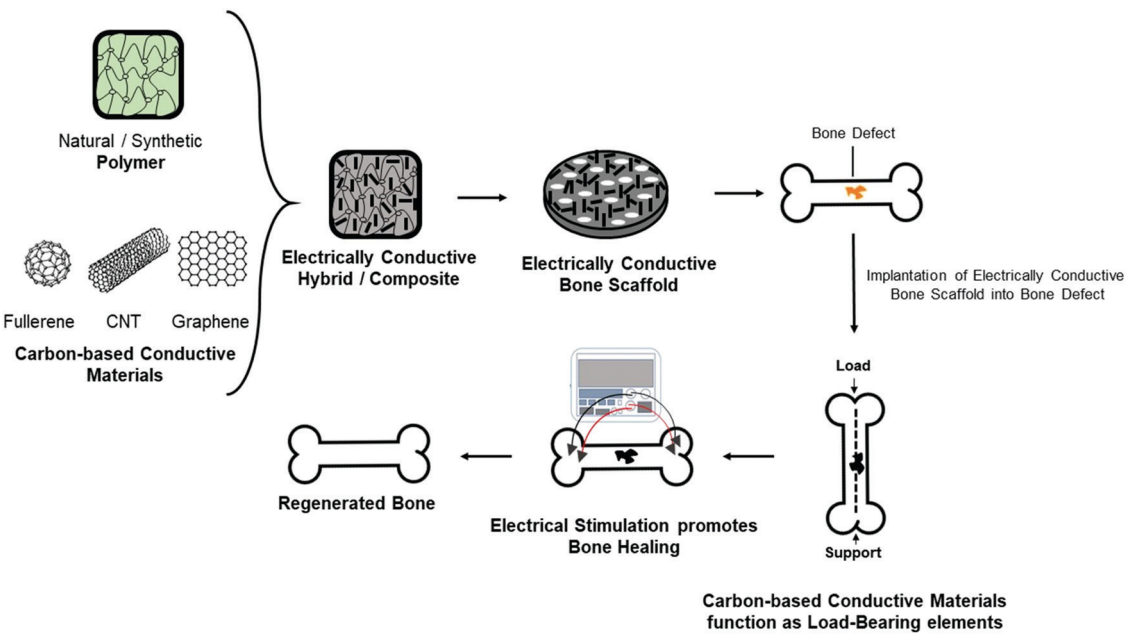

Fig. 1 Application of carbon-based conductive materials for bone repair and regeneration. Electrically conductive bone scaffolds are developed through the incorporation of carbon-based conductive materials into natural/synthetic polymers, creating a tissue-engineered bone that can be implanted into regions of bone defects. The aim of the implanted electrically conductive tissue-engineered bone is to degrade at a similar rate to the formation of new tissue to maintain the integrity of the repaired region while acting as a load-bearing element until the scaffold is completely remodeled and matches the original tissue's mechanical strength. Electrical stimulation can be delivered to the implanted conductive bone scaffold to promote cell proliferation, migration, and maturation of bone.

The incorporation of electrically conductive materials that enhance tissue restoration is a promising field within bioengineering and can be applied across various contexts. This is demonstrated by the recent articles that have reviewed the use of electrically conductive materials, including conductive polymers[23] to regenerate cardiac,[24] muscle,[25] and nerve.[26] However, a focused review of electrically conductive materials that can influence bone formation and their potential in clinical translation is lacking. Therefore, this review will discuss the importance of incorporating carbon-based conductive materials into bone scaffolds. The preparation strategies of different types of carbon-based conductive materials, including zero-dimensional buckminsterfullerene (C_{60}), one-dimensional carbon nanotubes (CNTs), and two-dimensional graphene-based sheets, will be presented. More specifically, we discuss the different applications of CNTs and graphene-based materials as they continue to be investigated for bone repair and regeneration. Lastly, the physiological responses of CNTs and graphene-based materials will be discussed for their potential as bone substitutes. Overall, this review aims to provide a better understanding of how carbon-based conductive materials, specifically one- and two-dimensional carbon-based materials, could potentially become promising candidates for bone tissue engineering solutions.

2. Electrical conductivity of native bone

The electrical conductivity of bone was discovered in the 1950s when Fukada and Yasuda observed that by applying mechanical stress to the bone in different directions, electrical signals were generated within the bone and they produced an endogenous electric field that supported osteogenic cell proliferation.[20,21,27] Since then, it has been suggested that stress on the crystalline components of bone produces current to flow and triggers healing and that electrical signals similar to those generated by mechanical stress can enhance fracture-healing.[28,29]

The endogenous electric field is generated by an applied mechanical load on the bone which creates strain gradients, and these strain gradients produce pressure gradients which in turn allow interstitial fluid to flow through small channels known as caniculae within the bone structure. Fluid flows from areas of compression to areas of tension within the stressed bone, and as a result, electrical potentials are generated (Fig. 2).[30] Electronegative potentials are developed upon compression, producing bone formation, whereas electropositive potentials are produced when a bone is under tension, causing bone resorption.[30,31] Therefore, administration of exogenous electrical stimulation at the site of a bone defect can be applied as a way to mimic the normal formation of electrical potentials generated on bone upon application of mechanical loads.

Since the discovery of electrically conductive properties of bone, various methods have been investigated clinically to deliver electrical stimulation in an attempt to aid bone healing

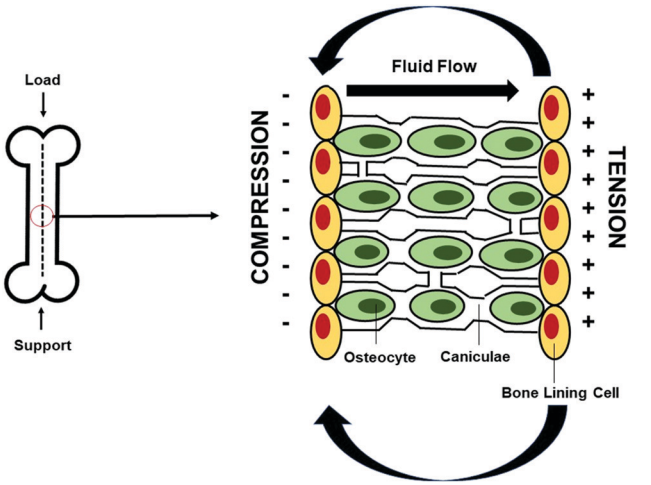

Fig. 2 Generation of electrical potentials through mechanotransduction in bone. Endogenous electrical potentials are generated in bone through the application of mechanical strain, during which interstitial fluid flows through the caniculae canals from areas of compression, generating electronegative potentials, to areas of tension, producing electropositive potentials. Bone formation is induced upon compression. Adapted from Duncan and Turner[30] (used with permission).

ranging from treatment of non-union,[32–34] bone fractures,[35,36] delayed unions,[37–39] osteotomies,[40,41] bone grafts with electrical stimulation,[42–44] and aiding of osteonecrosis.[45,46] Exogenous stimulation of bone healing can be delivered electrically through three main methods. The first approach is an invasive direct electrical current technique to stimulate bone whereby one or multiple cathodes are implanted onto the site of injury and an anode is implanted on soft tissue to permit current flow.[32,47,48] However, this technique carries a significant risk of infection and tissue reaction due to a lack of biocompatibility from the electrodes. Therefore, the two other alternative non-invasive techniques, namely, capacitive coupling and inductive coupling, have received significantly more attention in promoting bone healing. Capacitive coupling uses two electrodes that are placed onto the skin between the bone defects. The electrodes generate an alternating electric field which is delivered to the damaged site.[49,50] However, the need for a high voltage power source in this method is a major limitation since the energy dissipated from the electric field decreases quickly. In the alternative, inductive coupling uses non-invasive electromagnetic field stimulation.[51–53] In this method, one or two current-carrying coils are placed onto the skin, through which pulsed or sinusoidal electromagnetic fields are delivered that subsequently induce an electrical field in the damaged area.[54] Amongst these three techniques, inductive coupling best mimics the natural strain-generated potentials found in bone for its repair.[55,56] However, the principle behind all three techniques has made possible the development of medical devices that have received FDA approval[57,58] to stimulate bone electrically for its healing.[59,60]

Although electrical activity on bone defects promotes accelerated healing, there are some drawbacks, as mentioned above, related to the use of electrodes or the amount of energy

required to promote bone regeneration. However, incorporating a conductive material directly onto a polymer scaffold could potentially eliminate the requirement for electrodes and could allow the effects of electrical stimulation on bone regeneration to be explored. Electrically conductive materials are thus emerging for bone tissue engineering due to the natural conductive properties of bone. Although conducting polymers, such as polyaniline (PANI), polypyrrole (PPY), and polythiophene and their derivatives have also been used for bone tissue engineering applications,[16,61] carbon nanotubes (CNTs), graphene, and reduced graphene oxide (rGO) have received the greatest attention for application in bone tissue engineering solutions as they possess different geometrical and morphological structures that can alter their physiological responses and thus enhance their potential to function and treat bone defects.

3. Types of carbon-based conductive materials and their preparation strategies

Carbon-based conductive materials are divided into zero-dimensional buckminsterfullerene (C_{60}), one-dimensional carbon nanotubes (CNTs), and two-dimensional graphene sheets. Buckminsterfullerene (C_{60}), also known as fullerene or buckyball, are hollow spheres typically composed of 60 carbon atoms formed through a layer of stacked sp^2 hybridized carbon sheets arranged in hexagonal rings.[62] Buckyballs can exist in other forms and structures, such as ellipsoids or buckytubes, which are also known as carbon nanotubes (CNTs). CNTs are made from single atoms of sp^2 hybridized hexagonal carbon. A single atomic layer of a graphitic sheet can be rolled up into a single hollow cylinder creating a structure commonly referred to as single-walled CNTs (SWCNTs) with typical diameters ranging between 0.5 and 1.5 nm.[63] Alternatively, between 2 and 50 graphitic sheets can be rolled up into a coaxial tube with an outer diameter ranging between 2 and 100 nm forming multi-walled CNTs (MWCNTs).[63] A major feature of CNTs is that they possess unique mechanical, chemical, and electrical properties that resulted from their tubular shape and sp^2 hybridized C–C bonds.[64] Lastly, two-dimensional graphene is composed of a two-dimensional monolayer sheet of carbon in which the carbon atoms are sp^2 hybridized, containing σ bonds that create a lattice structure and conjugated π orbitals that form a delocalized electron network providing excellent conductive properties.[65,66]

Carbon-based conductive materials can be produced predominantly based on a technique in which gaseous carbon feedstock reacts in the presence of catalysts to form different shapes of carbon allotropes.[62,67] An example of this is buckyballs, which were first produced through laser ablation[68] and the process is later adapted for the synthesis of MWCNTs and SWCNTs in the presence of metal catalyst particles.[69–71] However, MWCNTs were first produced using arc discharge fullerene reactors,[72,73] and were later applied for the synthesis of SWCNTs.[74] Currently, the most affordable and scalable technique to produce CNTs is using chemical vapor deposition (CVD), during which a gaseous carbon precursor is thermally decomposed in the presence of metal catalysts and subsequently deposited inside a nanostructured tubing.[75,76] The scalability of this approach ensures the use of carbon-based materials and remains an attractive avenue in clinical-scale production. However, it is not the only method through which CNTs can be produced. CNTs and graphene can also be synthesized either using bottom-up or top-down approaches.[77] Bottom-up techniques include epitaxial growth,[78] pyrolysis,[79,80] and CVD[81] and operate based on the principle of depositing gaseous precursors, typically graphite, onto a substrate. Top-down approaches, however, involve breaking down graphitic layers until obtaining graphene and common techniques use exfoliation and reduction processes.[77,82,83]

Another set of popular graphene-based materials includes graphene oxide (GO) and its reduced form, reduced graphene oxide (rGO). GO is synthesized using Hummers' method, in which pristine graphene is first oxidized and then exfoliated to obtain graphene oxide (GO).[84–86] The resulting GO has many oxygen-containing functional groups bound to sp^3 carbons, thus containing both sp^2 and sp^3 hybridizations.[87] The change in hybridization reduces the electrical conductivity of GO *via* disrupting the conjugated structure, in turn blocking conductive connecting pathways between the sp^2 domains.[87] GO can be subsequently reduced to rGO *via* many different processes, including thermal annealing, electrochemical reduction, or chemical reduction. The reduction process removes oxygen-containing functional groups resulting in a higher conductivity than GO but lower conductivity than pristine graphene due to the remaining oxygen groups.[88]

The different preparation strategies of zero-dimensional fullerene, one-dimensional CNTs, and two-dimensional graphene sheets allowed the development of various carbon-based conductive materials that can be incorporated into different biomaterial systems to fabricate bone tissue engineering scaffolds. Their applications in bone repair and regeneration bring significant advantages, leading to the design of novel biomaterials that overcome some of the drawbacks of current bone repair materials (Table 1).

4. Relevant properties of carbon-based conductive materials for bone tissue engineering

4.1. Physicochemical properties of carbon-based conductive materials

An interesting feature of carbon-based conductive materials is their ability to strongly adsorb most organic compounds.[113] Incorporating carbon-based conductive materials into polymers or ceramics is thus beneficial in bone tissue engineering as carbon-based biomaterials have highly delocalized π-bonds on their surfaces and can adsorb proteins.[114] The addition of carbon-based conductive materials is an important factor in fabricating a tissue-engineered bone since the grafted scaffold

Table 1 Types of carbon-based conductive materials and their role in bone tissue engineering

Type of carbon-based conductive material	Biomaterial system	Role in bone tissue engineering
Fullerene	Polyhydroxylated fullerene (fullerol)[89]	Antioxidative capacity promotes osteogenic differentiation and mineralization[89]
	Polyethylene glycol (PEG)-functionalized C_{60} fullerene derivative[90]	Good biocompatibility and enhanced osteoblast proliferation[90]
	Aligned fullerene C_{60} nanowhiskers[91]	Good osteoblast adherence, aligned oriented cell growth, and low toxicity[91]
	GelMA-fullerol microspheres and bone marrow-derived mesenchymal stem cell (BMSC)-laden GelMA-fullerol microspheres[92]	Antioxidant activity is able to quench intra- and extracellular reactive oxygen species (ROS), promotion of osteogenic stem cell differentiation *in vitro* and bone healing in rat calvarial defects *via* modulating the ROS microenvironment[92]
CNTs	CNT-hydroxyapatite (HA) based nanocomposites[93]	Good biocompatibility[93]
SWCNTs	Functionalization of 3D-printed poly(propylene fumarate) (PPF) scaffolds with single-stranded deoxyribonucleic acid (ssDNA) bound CNTs[94]	Improved cell adhesion, proliferation, and differentiation of preosteoblast cells enabling modulation of cell behavior through electrical stimulation[94]
MWCNTs	SWCNT gel scaffolds with nanofibrous architecture *via* the pairing of heparin functionalized nucleobases[95]	Targeted drug delivery, increased mechanical properties, and improved osteogenic properties through the application of electrical stimulation[95]
	MWCNT compacts[96]	Induction of osteogenic gene expression, increased protein adsorption and mineralization, and the influence of ectopic bone formation[96]
	MWCNT-COOH reinforced borosilicate BG scaffolds[97]	Enhanced mechanical properties, bioactive behavior promoting hydroxyapatite formation, good cell viability, and osteogenic initiation[97]
	Chitosan-hydroxyapatite MWCNT nanocomposite films[98]	Biocompatible, electrically conductive, and good mechanical properties[98]
	Polycaprolactone (PCL)/MWCNT scaffolds[99]	Promotion of thick bone tissue formation *in vivo*, increased angiogenesis and mineralization of bone through electrical stimulation *in vivo*, and activation of osteoclastogenesis through electrical stimulation for bone remodeling[99]
	MWCNT reinforced polyvinyl alcohol/Biphasic calcium phosphate (PVA/BCP) scaffolds[100]	Increased mechanical properties, high interconnectivity, and good biocompatibility[100]
	Bionic mineralized MWCNT scaffolds[101]	Improved mechanical properties, enhanced cell growth *in vitro* and *in vivo*, increased osteogenic differentiation and promotion of bone defect repair *in vivo*[101]
Graphene	Hyaluronic acid–chitosan with simvastatin[102]	Biocompatible and bioactive 3D scaffold with improved osteogenic properties[102]
GO	rGO coated collagen scaffolds[103]	Enhanced mechanical properties, good biocompatibility, and proliferation of human bone marrow-derived mesenchymal stem cells (hBMSCs), and increased bone formation after implantation into cranial bone defects in an animal model[103]
rGO	Graphene hydrogel membrane[104]	Guided bone tissue regeneration in a rat calvarial model, diffusion of proteins and nutrients, and promotion of early osteogenesis and mineralization to induce mature bone formation *in vivo*[104]
	Gelatin methacrylate, acryloyl-β-cyclodextrin, and β-cyclodextrin-functionalized rGO nanocomposite hydrogel patch[105]	Improved mechanical strength, increased conductivity, good biocompatibility, promotion of cell proliferation and osteogenic differentiation, and enhanced *in vivo* bone defect repair in a rat skull model[105]
	Vascularized GO-collagen chamber model[106]	Improved bone regeneration *in vivo*, osteoinductive properties and anti-fibrosis effects in an animal model, and improved angiogenic, mineralization and osteogenic differentiation of BMSCs[106]
	GO-modified silk fibroin/nanohydroxyapatite scaffold loaded with urine-derived stem cells (SCs)[107]	Immunomodulation and promotion of bone regeneration *in vivo*, and enhanced mechanical properties[107]
	Polylactic acid (PLA)/GO nanocomposite 3D scaffolds[108]	Enhanced mechanical properties, good biocompatibility and promotion of cell proliferation and mineralization[108]
	Graphene/hydroxyapatite nanoparticle composite hydrogels[109]	Mechanically strong, electrically conductive, and biocompatible[109]
	Collagen-rGO coated scaffolds[110]	Improved mechanical properties and enhanced osteogenic capability[110]
	rGO-coated titanium substrates[111]	Promotion of the osteogenic differentiation of hMSCs and increased calcium phosphate deposition and osteogenic potential[111]
	3D-printed β-tricalcium phosphate (TCP)-based scaffolds filled with a freeze-dried gelatin/rGO-magnesium–arginine matrix[112]	Enhanced mechanical properties, improved cell proliferation and osteogenic differentiation[112]

can interact with the host tissue through the protein absorption properties of the materials permitting osteogenic progenitor cells to adhere, implant, and begin to lay down their extracellular matrix (ECM).[8] The establishment of a new ECM is the critical first step in scaffold remodeling and bone tissue regeneration. Adsorption of proteins onto CNTs and graphene surfaces is mediated by several different variables, including the geometry of carbon-based conductive materials and the formation of non-covalent interactions.[114,115] The non-covalent interactions or physical adsorption of proteins with carbon-based conductive materials involves the presence of different binding selectivity which is governed by the formation of hydrophobic interactions, π–π stacking interactions (van der Waals forces and dispersion forces), electrostatic interactions, and H–π bonds.[114,116,117]

Hydrophobic interactions occur due to the great affinity of the hydrophobic regions of cell-binding proteins with the hydrophobic carbon lattices present in the conductive material.[118] Protein adsorption on CNTs and graphene surfaces strongly depends on the electron density and geometry of protein molecules.[119] In the case of π–π stacking interactions, binding interactions occur when the aromatic side chains of amino acids are oriented parallel with the plane of carbon-based conductive materials at different charge states.[115,120] Peptides possess different aromatic side chains resulting in different polarizability properties, which, in turn, influence the strength of binding with carbon-based conductive materials. In general, the higher the polarizability of the protein aromatic side chains, the greater the binding strength. Polarizability of aromatic protein side chains is in the increasing order of His < Phe < Tyr < Tryp.[121–123]

Another non-covalent interaction is electrostatic binding, which forms in the presence of different charges between cellular proteins and carbon-based conductive materials. Surface charges vary in carbon-based conductive materials due to the type of product synthesized and the variation in the preparation procedures. As an example, GO is a material with a surface rich in negatively charged oxygenated functional groups. The strong negative charge generated by these groups facilitates GO binding with proteins that have either negatively or positively charged surfaces resulting in electrostatic interactions with various degrees of stability.[114] The importance of material surface structure and functionalization was demonstrated in a study by Chong *et al.*,[124] in which the strength of protein interactions with various carbon-based conductive materials was assessed.[124] The study revealed that GO and rGO have increased ability to adsorb proteins compared to SWCNTs because it is easier for proteins to bind onto the planar surfaces of graphene compared to the curved surfaces of CNTs.[124]

Incorporation of a carbon-based conductive material into a bone tissue engineering scaffold could be beneficial for bone defect treatments since their ability to adsorb proteins allows osteoblasts to attach to the bone scaffold. This step appeared to be crucial for the remodeling and regeneration of bone tissue and as demonstrated in the following studies. Taale *et al.*[125] developed bioactive carbon-based hybrid 3D scaffolds composed of either CNT-bioactive glass nanoparticles (BGN) or CNT-hydroxyapatite (HA) nanoparticles to assess their protein adsorption capacity using bovine serum albumin (BSA) as a model protein.[125] This study revealed that CNT-BGN had higher protein adsorption ability than CNT-HA scaffolds due to a plausible electrostatic interaction between the high polarity of BSA and the BGN surface etching/sintering process to remove a sacrificial ZnO template.[125] Similarly, Fu *et al.*[126] incorporated GO into poly(L-lactic-*co*-glycolic acid) (PLGA)/HA nanofiber scaffolds and observed that the addition of carbon-based conductive materials significantly increased the protein adsorption (Fig. 3A).[126] PLGA/GO/HA nanofibrous matrices obtained the highest protein adsorption rate of nearly 1.46 and 1.25 times that of PLGA/HA and PLGA/GO nanofibrous matrices, respectively, since the addition of GO and HA improved the surface properties, resulting in higher specific surface areas.[126] Using materials that increase protein adsorption can therefore promote cell adhesion and proliferation of preosteoblasts, enhancing bone maturation and mineral deposition.[126] Du *et al.*[127] compared the osteogenic ability of MWCNTs and nanohydroxyapatite (nHA), the main inorganic component of bone, and showed that MWCNTs are more effective materials for the promotion of bone formation.[127] The results showed that MWCNT compacts possessed higher ability to adsorb fetal bovine serum (FBS) proteins than nHA (Fig. 3B). High protein adsorption ability had a positive effect in further *in vitro* studies revealing that human adipose-derived mesenchymal stem cells cultured on MWCNT compacts possessed a higher cell attachment strength and proliferation than nHA specimens.[127] In addition, MWCNTs could induce osteogenic differentiation better than nHA since an increased protein concentration modulates the conformation of the adsorbed proteins driving the differentiation of cells toward an osteoblastic lineage by the activation of Notch signaling pathways.[127] Translation of *in vitro* results was further investigated in a rabbit model, where both MWCNTs and nHA compacts were implanted in dorsal musculatures. The results showed that MWCNT compacts were able to induce ectopic bone formation while nHA did not (Fig. 3C) as a result of the increased ability of MWCNT compacts to adsorb proteins and drive the formation of new bone tissue.[127]

4.2. Electrical properties of carbon-based conductive materials

Human cortical and cancellous bone have electrical conductivities of 0.02 S m^{-1} and 0.07 S m^{-1}, respectively.[128] CNTs and graphene are two of the most attractive materials that are being used in scaffolds for bone repair and regeneration applications[97–99,103,105,107,111] as they possess very high electrical conductivities of 10^6–10^7 S m^{-1} for pure CNTs and 10^8 S m^{-1} for pure graphene.[129] Therefore, hybrid bone scaffolds containing a low amount of CNTs or graphene can result in a conductivity that recapitulates endogenous bone. The high conductivity of carbon-based conductive materials is a result of their basic microstructural element in which a 2D

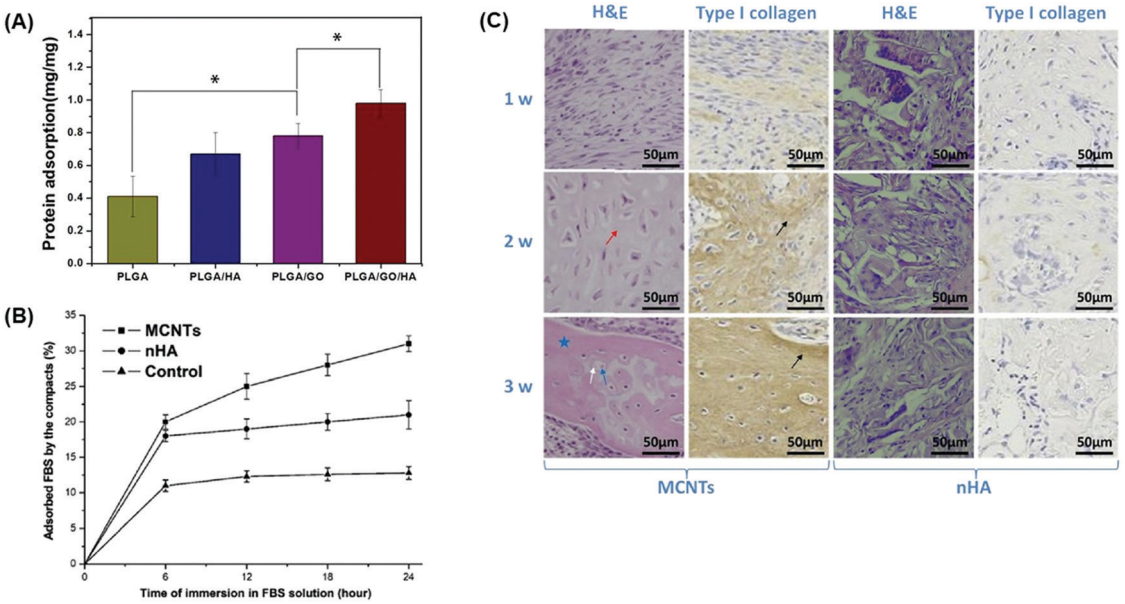

Fig. 3 Protein adsorption ability of bone tissue engineering scaffolds containing GO and MWCNTs promotes bone formation. Different carbon-based conductive materials have been incorporated into bone scaffolds to test their protein adsorption efficiencies, which can subsequently drive bone differentiation and maturation. (A) Protein adsorption efficiencies of nanofibrous matrices composed of PLGA, GO, and HA were assessed after 24 h using BSA as a model protein. Materials containing GO displayed the highest level of protein adsorption.[126] (B) Protein adsorption in compacts composed of either MWCNTs or nHA in an FBS protein model at increasing time points. Compacts containing MWCNTs displayed higher ability to adsorb proteins than those composed of nHA.[127] (C) *In vivo*, compacts containing MWCNTs implanted into the rabbit dorsal muscle pouch displayed higher levels of new bone and collagen formation as evidenced by hematoxylin and eosin (H&E) and type I collagen staining that is not observed in the nHA compacts[127] (used with permission).

single-layered graphene sheet is arranged in a honeycomb grid of carbon atoms possessing four electrons in the outer shell, three of them are used for covalent bonds while the remaining electron is highly mobile promoting electrical conduction.[130] Therefore, the electrical conductivity of bone scaffold composites is more appropriately explained in terms of the percolation threshold.

The percolation threshold is related to the addition of a critical volume fraction of conductive filler within a hybrid material that results in the transition from an insulating state to a significant change in the overall electrical conductivity caused by the formation of a continuous network of conductive particles within the insulating matrix.[131] The percolation threshold is described by an empirical model known as scaling law, expressed as $\sigma(\Phi) = \sigma_0(\Phi - \Phi_c)^t$ where Φ_c is the percolation threshold concentration and t is the critical exponent.[132] Below the critical volume fraction of the percolation threshold, the conductivity of the composite remains electrically insulating since the conductive particles are dispersed into small clusters. Above the critical volume fraction, however, the material no longer behaves as an insulator, and its conductivity increases by many orders of magnitude.[131] The aspect ratio of the conductive fillers determines the percolation threshold value. Graphene and CNTs have a length-to-diameter aspect ratio of 0.01 and 100, respectively, which differs due to their different geometrical structures.[129] Therefore, hybrid bone biomaterials containing a low amount of carbon-based conductive materials can significantly increase the overall electrical conductivity, thus requiring a small amount of filler to achieve the percolation threshold.[129]

The advantages of incorporating a carbon-based conductive material directly onto a polymer bone scaffold could, in principle, eliminate the requirement for electrodes that are normally used for the treatment of bone defects since they possess electrically conductive properties (Fig. 4). Cells are responsive to exogenous electric fields and have been shown to promote key signaling pathways that accelerate osteogenesis and angiogenesis, the main processes for bone regeneration and remodeling, upon application of different field strengths and current densities.[43,133] *In vitro* studies have shown that the application of electrical stimulation through direct, capacitive and inductive coupling induces key molecular pathways at different cellular locations involved in osteogenesis, specifically through the calcium/calmodulin pathway, resulting in minor alternative cellular responses (Fig. 5A).[43,134] Direct and capacitive coupled stimulation exerts their effects on the cell membrane, increasing the intracellular Ca^{2+} concentration and prostaglandin E2 synthesis through calcium translocation *via* voltage-gated calcium channels.[135] Moreover, inductively coupled stimulation through electromagnetic fields achieves its effects in the cytoplasm where intracellular calcium accumulation is released from reservoirs, such as the endoplasmic reticulum.[136] Application of these exogenous stimulations results in cellular responses that increase calcium concentration, thus promoting activated calmodulin levels to drive osteoblast cell proliferation, as well as an increased expression of vascular

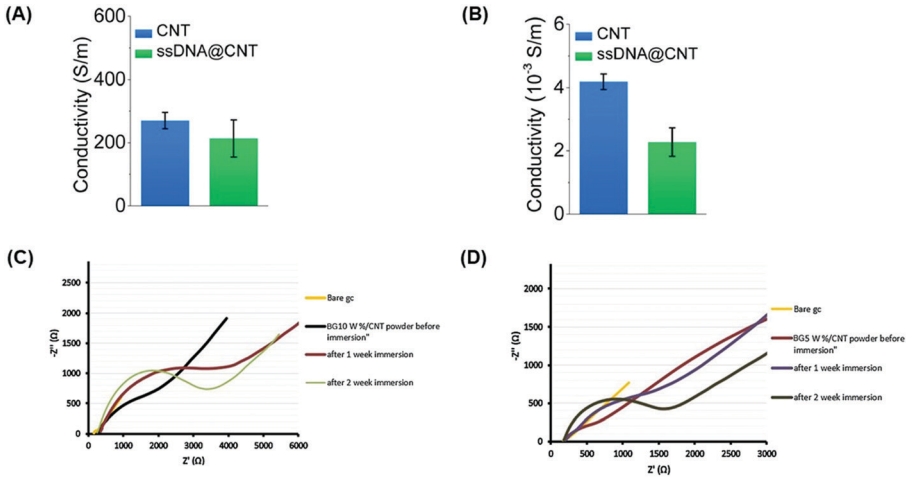

Fig. 4 Carbon-based conductive materials incorporated into bone tissue engineering scaffolds possess electrically conductive properties, eliminating electrodes in bone healing treatments. Carbon-based conductive materials have been incorporated into bone scaffolds and tested for their electrical properties. Electrical conductivities of CNTs and CNTs with water-soluble single-stranded deoxyribonucleic acid (ssDNA) (ssDNA@CNT complex) were tested both in solution at a concentration of 0.5 mg ml^{-1} (A) and in solid-state in the form of pellets (B).[94] Electrochemical impedance of (C) BG/10 wt% CNT and (D) BG/5 wt% CNT powders before and after immersion in simulated body fluid (SBF) for one and 2 weeks were measured[17] (used with permission).

endothelial growth factor (VEGF) and transforming growth factor (TGF)-β1.[134,137,138]

The addition of carbon-based conductive materials into bone tissue engineering scaffolds improves the effects of the bone regeneration rate through electrical stimulation.[95,108,139,140] Injectable conductive hydrogels have gained significant attention in bone tissue engineering since they can be delivered into irregular bone tissue defects while guiding new bone formation.[141–143] As demonstrated in a study by Liu *et al.*,[144] an injectable conductive hydrogel, BP-CNTpega-gel, composed of CNT-poly(ethylene glycol)-acrylate (CNTpega) with black phosphorous (BP) was developed to support bone regeneration.[144] The inclusion of CNT as the conductive component in the hydrogel allowed BP-CNTpega-gel to possess electrically conductive properties. The highest conductivity value reported was 0.008 S m^{-1} at a CNTpega concentration of 16 mg ml^{-1} and a BP nanosheet concentration of 0.8 mg ml^{-1}.[144] Furthermore, *in vitro* studies showed that hydrogels with CNTpega effectively respond to exogenous electrical stimulation resulting in increased cell proliferation and ALP activity, as well as an upregulation of osteogenic genes and bone mineralization markers (Fig. 5B–E).[144] In another study, 3D conductive scaffolds composed of polycaprolactone (PCL) and MWCNTs (0.75 wt% and 3 wt%) were developed by e Silva *et al.*[99] to treat large calvarial bone defects in rats.[99] Conductive scaffolds were produced through extrusion-based additive manufacturing and cut to fit the bone defect in animal skull models (Fig. 5F).[99] The authors applied non-invasive electrical stimulation to the grafted region for 5 min at 10 μA intensity twice a week for a 60 or 120 day period. Prolonged stimulation at this frequency was considered appropriate for future clinical trials in potential long-term treatment patients.[99] Histomorphometry results from the study showed that thicker tissue formation was observed in treatment groups that contained scaffolds than in the untreated groups. Furthermore, the groups treated with PCL scaffolds containing 3 wt% MWCNTs and additionally underwent electrical stimulation showed elevated connective and denser bone tissue formation (Fig. 5G).[99] Therefore, incorporating MWCNTs into PCL scaffolds and applying electrical stimulation significantly promoted angiogenesis and mineralized bone tissue formation.[99] Similar findings have also been reported in 3D printed PCL/graphene scaffolds in a rat calvarial bone defect model.[145] New bone tissue formation was most effective with scaffolds containing graphene and electrical stimulation *in vivo*, leading to organized tissue deposition and bone remodeling.[145] Collectively, these studies demonstrate the translational potential for clinical approaches combining conductive materials into bone scaffolds and electrical stimulation for accelerated repair and regeneration of bone defects.

4.3. Mechanical properties of carbon-based conductive materials

The mechanical properties of carbon-based conductive materials can greatly influence their application and function in different types of biomaterials. CNTs and pristine graphene have different mechanical properties (Table 2) due to their varied morphological and geometrical structures but possess excellent mechanical strength of approximately 100 times greater than that of steel, but with an extremely low density (1.3–2.0 g cm^{-3}) compared to metals or ceramics (>2.0 g cm^{-3}).[146] The high mechanical and tensile strength of CNTs set them apart from other carbon-based materials. In comparison to GO and rGO, both CNTs and graphene possess mechanical strengths greater than that of GO and rGO. GO and rGO monolayers possess a Young's Modulus of 207.6 ± 23.4 GPa and 250 ± 150 GPa, respectively.[147,148] The lower strength of GO and rGO is predominantly due to the chemical processes used in their production which decrease their stability originating from the sp^2 bond that forms the hexagonal

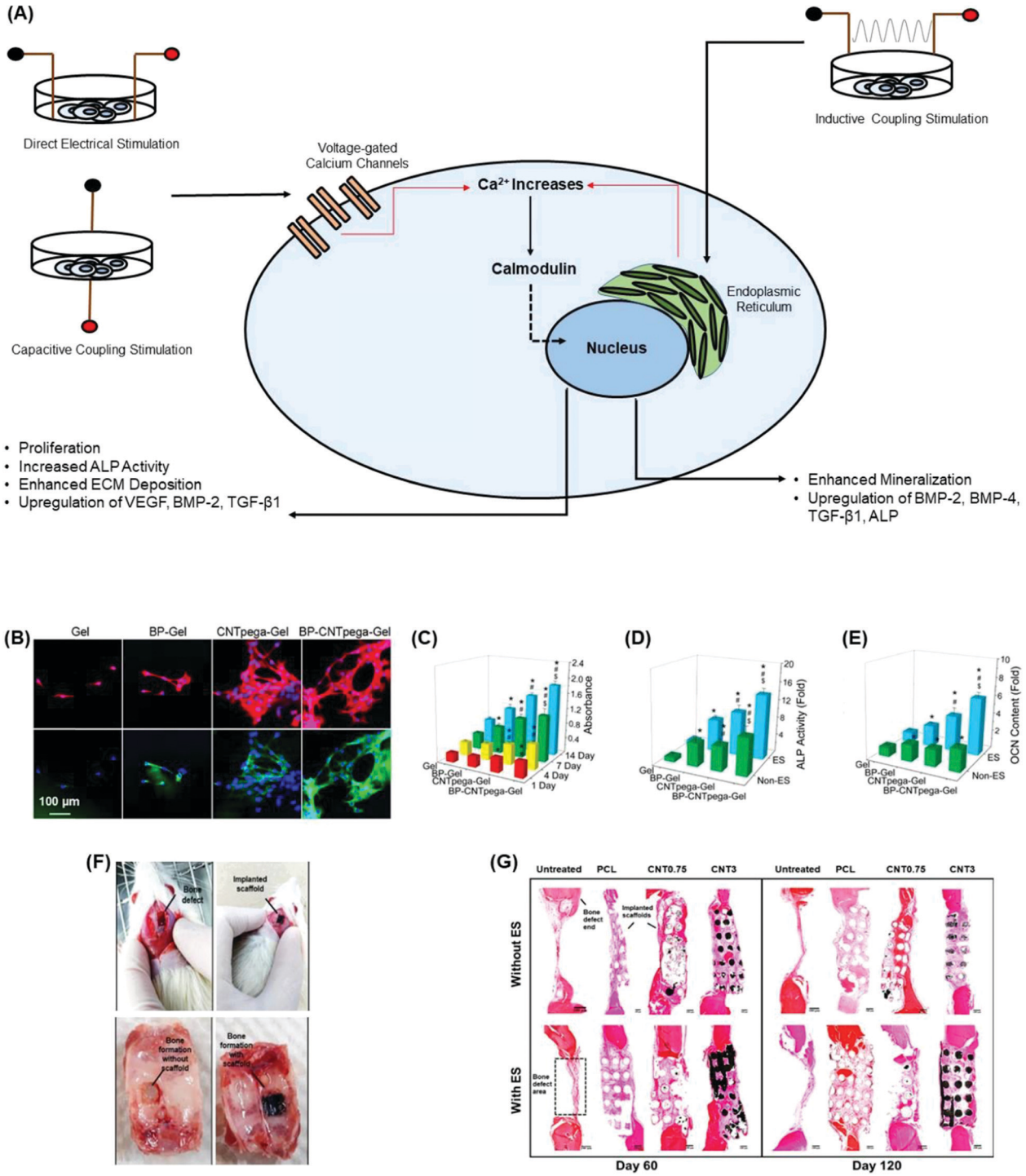

Fig. 5 Incorporation of carbon-based conductive materials into bone tissue engineering scaffolds promotes osteogenesis and *in vivo* bone formation. (A) Cellular response of different electrical stimulation techniques promotes osteogenesis through the activation of the calcium/calmodulin pathway.[134] (B) Immunofluorescence staining images on MC3T3-E1 preosteoblasts show a cellular response upon the application of electrical stimulation after 7 days post-seeding. Cells were largely elongated and stretched in cell shape.[144] (C) Cell proliferation under electrical stimulation was evaluated using hydrogels at 1, 4, 7, and 14 days post-seeding. On days 1 and 4, CNTpega-gels and BP-CNTpega-gels showed significantly higher cell numbers than BP-gels and oligo(poly(ethylene glycol)fumarate) (OPF) as the control.[144] BP-gels, CNTpega-gels and BPCNTpega-gels showed significantly higher cell numbers than OPF on day 7. However, BP-CNTpega-gels had the highest cell density.[144] (D) Intracellular ALP activity was assessed in cells grown on hydrogels with or without electrical stimulation after 14 days of culture. Cells grown on BP-CNTpega-gels possessed the highest ALP activity.[144] After treatment by electrical stimulation, ALP activities increased for all hydrogels; however, the highest increase in ALP activity was shown in cells grown on BP-CNTpega-gels.[144] (E) Determination of the osteocalcin (OCN) content in cell culture media after 21 days of culture with and without electrical stimulation. OCN was significantly higher in cells grown on BP-CNTpega-gels in the presence of exogenous stimulation, indicating potential mineralization enhancement.[144] (F) Image of the bone defects in a calvarial animal model as well as the implanted PCL/MWCNT scaffold. Subsequent bone tissue formation with and without the scaffold was obtained on day 60 post-implantation.[99] (G) The cross-sections of bone tissue regeneration at the bone defects for untreated, PCL and PCL/MWCNT (0.75 wt% and 3 wt%) groups after 60 days and 120 days post-operation.[99] PCL/MWCNT 3 wt% subjected to electrical stimulation formed the highest connective and bone tissues on days 60 and 120[99] (used with permission).

lattice.[149] Mechanical strength is considered one of the most crucial properties in the preparation of a scaffold for bone tissue engineering applications. It is imperative that an implanted scaffold is strong enough to initially withstand the load that the bone tissue would have carried, but it gradually decreases as it is being remodeled by new tissue that eventually takes over the load. Therefore, it is important to know the mechanical properties of different types of bone (Table 2) in order to establish what concentration of the carbon-based conductive material is necessary to design a bone substitute that can support the natural mechanical strength of the defective bone region prior to its regeneration.

Carbon-based conductive materials can be used by themselves, but given their overall higher mechanical properties, stress shielding will likely cause bone resorption. Instead, they are incorporated into polymers as secondary structural reinforcing agents to increase the mechanical properties of two- and three-dimensional polymeric bone scaffolds. The unique structures and properties of carbon-based conductive materials provide an ideal solution for creating a bone scaffold that better matches the mechanical properties of natural bone tissue compared to previously explored polymeric-based scaffolds.[160–163]

In a study by Lu *et al.*,[104] a multilayered graphene hydrogel (MGH) membrane was developed to investigate whether the biomaterial possessed the ability to guide bone tissue regeneration in a rat calvarial model.[104] Within the regenerating region, diffusion of proteins and nutrients took place through the selective permeability of the MGH membranes promoting early osteogenesis and mineralization which resulted in the formation of a mature bone structure surrounded by external and internal cortical bone after eight weeks of implantation.[104] Although MGH membranes are very flexible, they maintain mechanical strength similar to that of a rat braincase with a tensile modulus of 69 $\pm$ 5 MPa.[104]

The mechanical strength of a biomaterial can be modulated by altering the proportion of carbon-based material in the final composition. This principle was demonstrated in a study by Belaid *et al.*[108] which investigated biocompatible polylactic acid (PLA)-based scaffolds produced by 3D printing and the effect of incorporating different concentrations of GO (0.1, 0.2, and 0.3 wt%) as a reinforcement element for bone healing applications.[108] Pure PLA scaffolds presented a Young's modulus of 2 GPa, but this was significantly increased to 2.6 GPa upon the addition of 0.3 wt% GO (Fig. 6A).[108] In addition, materials containing 0.3 wt% GO presented the highest tensile strength with a value of 39 MPa, whereas pure PLA presented the lowest tensile strength of 34 MPa (Fig. 6B).[108] However, GO concentrations of 0.1 and 0.2 wt% showed a decreased tensile strength compared to 0.3 wt% GO since a lower filler concentration induced flaws at a local scale resulting in a weaker material.[108] Therefore, at higher GO concentrations, the filler is intrinsically stronger than PLA, resulting in a stronger material.[108]

Qian *et al.*[95] developed a CNT gel scaffold that contained functionalized nucleobase pairing for targeted drug delivery and *in vitro* osteogenesis.[95] The conductive gel scaffold was prepared by functionalizing heparin (HP) with adenine (HP-A) and thymine (HP-T) which were subsequently grafted to aminated CNTs forming CNT-HP-A and CNT-HP-T precursors.[95] The mixture of these precursors resulted in a nucleobase paired CNT gel network. Dynamic time sweep rheological tests were performed in order to investigate the gel network evolution during the gelation process at 37 °C. The results showed that the CNT-HP-A/CNT-HP-T mixture formed a dynamic network within less than 5 min which was shown by the crossover of storage modulus (G') and loss modulus (G'') (Fig. 6C).[95] In addition, after 14 min a structurally stable network was formed for both CNT and control (HP-A/HP-T) gels, reaching a G' value of around 100 Pa which could translate to the successful development of gels capable of maintaining their 3D shape for therapeutic drug loading purposes.[95] The structural integrity of the scaffold gels was also evaluated through compressive tests, and results were compared before and after loading with bone morphogenetic protein 2 (BMP-2) as a potential osteogenic drug loading model.[95] The compressive modulus of scaffold gels containing CNTs was significantly higher (256 kPa) than that of HP-A/HP-T gels (83 kPa).[95] Loading of gels with 50 ng ml^{-1} BMP-2 did not affect the overall compressive strength of the gels, but CNT-containing scaffolds presented a final modulus value of 264 kPa (Fig. 6D).[95] Furthermore, Bahrami *et al.*[103] prepared rGO coated collagen (Col-rGO) scaffolds by chemical crosslinking and freeze-drying methods to assess their mechanical strength for implantation into rabbit

Table 2 Comparison between the mechanical properties of carbon nanotubes, pristine graphene monolayer, and cortical and cancellous bone

Carbon nanotubes	Tensile strength	10–200 GPa[150–152]
	Compressive strength	~1 GPa[153]
	Young's modulus	0.27–1.47 TPa[152,154]
	Surface area	50–1315 m^2 g^{-1} [146]
Pristine graphene monolayer	Tensile strength	130.5 GPa[155]
	Compressive strength	~416 MPa[156]
	Young's modulus	1 TPa[157]
	Surface area	2391–2630 m^2 g^{-1} [158]
Cortical bone	Tensile strength	50–150 MPa[159]
	Compressive strength	100–230 MPa[159]
	Young's modulus	7–30 GPa[159]
Cancellous bone	Tensile strength	10–20 MPa[159]
	Compressive strength	2–12 MPa[159]
	Young's modulus	0.5–0.05 GPa[159]

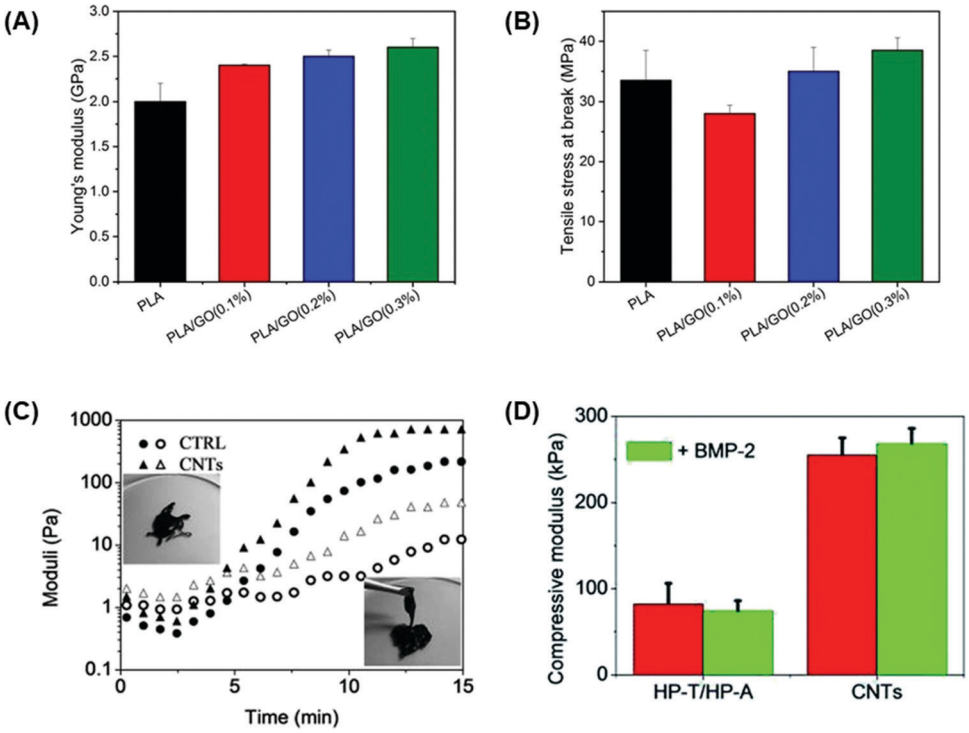

Fig. 6 Carbon-based conductive materials enhance the mechanical strength of bone tissue engineering scaffolds. (A) Young's modulus and (B) tensile strength at break of pure PLA scaffolds and PLA scaffolds containing 0.1, 0.2, and 0.3 wt% concentrations of GO as a reinforcement filler.[108] Higher concentrations of GO increased the mechanical properties of the PLA-based scaffolds.[108] (C) Dynamic time sweep rheological tests were performed on HP-A/HP-T control and CNT-HP-A/CNT-HP-T to assess the gel network evolution at 37 °C.[95] A dynamic network was formed in the CNT-HP-A/CNT-HP-T mixture within less than 5 min which was shown by the crossover of the storage modulus (G': filled symbols) and loss modulus (G'': open symbols).[95] (D) Compressive modulus of HP-A/HP-T control and CNT-HP-A/CNT-HP-T with or without BMP-2 loading at 37 °C.[95] The compressive modulus of the scaffold gels containing CNTs was significantly higher than control gels, especially with BMP-2 loading[95] (used with permission).

cranial bone defects.[103] Compressive tests were performed on collagen and Col-rGO scaffolds to evaluate the elastic modulus of the scaffolds.[103] Col-rGO scaffolds showed an elastic modulus of 325 ± 18 kPa, whereas pure collagen scaffolds presented a modulus of 115 ± 16 kPa, which is not sufficient for rabbit cranial bone structural support.[103] The addition of coated rGO on collagen scaffolds not only increased the mechanical strength of the material but enhanced the cell viability and proliferation which translated into increased *in vivo* bone formation after 12 weeks of implantation into rabbit cranial bone defects.[103]

5. Cellular processing mechanisms of carbon-based conductive materials

Ideally, bone scaffolds should degrade at a similar rate to the formation of new tissue to maintain the integrity of the repaired region of bone, which can physiologically and mechanically adapt to the natural environment and local load within the body.[8,11] Although carbon-based conductive materials can be degraded through enzymatic oxidation using horseradish peroxidase, or hydrolytically through lipases,[164,165] the complete degradation and fate of CNTs and graphene-based materials in the body are still relatively unknown. However, *in vitro* and *in vivo* studies have shown that a variety of cell types such as macrophages,[166–168] endothelial cells,[169] pulmonary epithelia,[170,171] intestinal epithelia[172] and neuronal cells[173] can degrade and take up carbon-based conductive materials. Therefore, understanding how carbon-based conductive materials in bone scaffolds are processed and degraded by the specialized cell types they will interact with will be important for establishing safety in clinical translation.

In vitro studies have shown that carbon-based conductive materials can be internalized by cells; this movement is promoted by the hydrophobic interaction between the material and cell membrane imparted by the phospholipid bilayer.[174–176] However, cellular internalization is still reliant either on passive or active transport pathways present on the cell membrane. Passive diffusion transport is a non-energy-dependent process in which carbon-based conductive materials land on the surface of cell membranes and penetrate the phospholipid bilayer, resulting in subsequent transport into the cytoplasm.[176,177] On the other hand, the active pathways are energy-dependent processes and mainly occur through endocytic mechanisms that control the internalization of foreign objects from the cell membrane into cytoplasmic organelles called lysosomes, which can break down the extracellular material.[176,178] Although temperature and metabolic inhibitors potentially influence endocytosis, no factors have

been identified to date that governs the method or rate at which carbon-based conductive materials are internalized into cells.[176,179] Lacerda *et al.*[180] investigated the uptake mechanism of functionalized MWCNTs (f-MWCNTs) in the presence of cell uptake inhibitors at different temperatures and concluded that there was no single mechanism responsible for the transportation of CNTs into cells since 30–50% of f-MWCNTs were internalized into the cells through an energy-independent pathway, but the remaining f-MWCNTs entered the cells through endocytosis.[180]

The diameter of the conductive nanomaterial appears to be a critical factor in determining degradation post-internalization. Several studies have reported that small agglomerates of carbon-based conductive materials are more easily degraded in macrophages through lysosomal and endosomal activity,[175,181,182] in contrast to larger agglomerates of carbon-based conductive materials that are expelled from the cell through exocytosis.[183,184] Once internalized, materials on the nanoscale can migrate to other subcellular organelles.[185,186] This internalization of materials into cells and subsequently through the subcellular compartments was first demonstrated by exposure of human monocyte-derived macrophages to SWCNTs ranging from 0.6–3.5 nm in diameter.[185,186] In these studies, SWCNTs were observed to be localized solely within lysosomes two days after exposure, however after four days, they were observed to have crossed the nuclear membrane, as nanoparticle sizes of less than 40 nm can enter the nuclear pore complex.

In addition to the diameter, the configuration of carbon-based materials can also influence how they are processed cellularly. Work by Mu *et al.*[187] showed that single MWCNT–COOH and MWCNT–NH_2 (20–30 nm diameter and $\sim$1000 nm average length) were transported into human embryonic kidney epithelial cells (HEK293) through direct passive diffusion, whereas bundled MWCNTs entered cells through endocytosis.[187] The bundled MWCNTs were also subsequently processed and could release single MWCNTs capable of endosomal escape and release into the cytoplasm. Furthermore, those released single MWCNTs of shorter length were also capable of achieving nuclear translocation.[187]

Internalization, degradation, and externalization of carbon-based conductive materials need to be further investigated in osteoblasts and *in vivo* bone defects in order to understand their impact on bone tissue engineering applications and targeted bone drug delivery. In addition, migration of carbon-based conductive materials from bone scaffolds could occur as the scaffold is being remodeled and it is imperative to investigate whether their translocation causes any toxic or adverse effects.

Processing techniques used to synthesize carbon-based conductive materials influence the physicochemical properties of the material, causing different potential toxicological interactions.[188] Of key concern within the field is the potential of a carbon-based conductive material to generate reactive oxygen species (ROS), which can cause subcellular damage to organelles and processes, ultimately resulting in cell toxicity.[189] Catalytic metal impurities left over from the material processing are suggested to be one of the main reasons why ROS are formed.[190] The metal catalysts used during synthesis can remain attached to carbon-based conductive materials which can subsequently influence intracellular calcium concentrations, activate transcription factors, and modulate cytokine production *via* the generation of free radicals creating ROS and thus inducing acute toxicity.[191] However, carbon-based conductive materials can undergo various treatments to achieve higher purification to reduce potential metal particles that induce ROS formation. Treatments include chemical selective oxidations and dissolution of metallic impurities or physical purifications that involve the separation of impurities through their physical sizes and aspect ratios.[192]

In addition to impurities, the sizes of carbon-based conductive materials can influence the immunological effects in cells. Yoon *et al.*[193] showed that smaller graphene nanoflakes (30.9 $\pm$ 5.4 nm) have higher uptake affecting the cell membrane function, thus inducing apoptosis compared to larger graphene nanoflakes (80.9 $\pm$ 5.5 nm) which were shown to be less toxic given that they were mostly aggregated on the cell membrane.[193] The effects of the length and diameter of CNTs have also been shown to impact toxicity, where shorter CNTs (sub-1 μm) can easily penetrate into cell membranes and internalize, thereby accumulating in cell lysosomes,[194] whereas longer CNTs ($>$8 μm in length and $<$1.25 μm in diameter) are not engulfed into cell membranes and degraded causing acute inflammation increasing the production of ROS and cytokines thus exerting more significant biological effects.[195] However, Zhang *et al.*[196] showed that larger CNTs were taken up by macrophages and that the rope-like structures of CNTs had similar properties to spherical nanoparticles where cytotoxicity increased upon a higher internalization concentration of CNTs causing cell death with levels above 20 pg per cell.[196] Another factor that influences cytotoxicity is the dose of carbon-based conductive materials to cells. The effects of pristine GO concentrations on the viability of bone mesenchymal stem cells (BMSCs) were investigated, which showed that high concentrations (10 μg ml^{-1}) of GO inhibited the proliferation of BMSCs, while low concentrations (0.1 μg ml^{-1}) enhanced the cell proliferation.[197] Similar behavior was observed in biphasic calcium phosphate (BCP) coated with different concentrations of rGO; osteoblast viability was maintained above 80% at concentrations below 62.5 μg ml^{-1}, but significantly decreased at concentrations above 100 μg ml^{-1}.[198]

Ultimately, the aim of designing tissue engineering scaffolds containing carbon-based conductive materials is to utilize them for clinical translation. Therefore, understanding the cellular processing mechanisms that one- and two-dimensional carbon-based conductive materials undergo and the factors that influence their performance is important. Preclinical studies have shown that carbon-based conductive materials can be excreted *via* the kidneys and urinary tract after intravenous injection when graphene sheets are well dispersed and CNTs have a high degree of disaggregation.[199–202] These studies also provided evidence that the excretion of carbon-based conductive

materials from the body is dependent on size and shape. Although CNTs of dimensions over 2000 nm length and over 30 nm diameter,[201] and GO sheets of over 5 nm thickness[202] accumulated in the liver and spleen, they showed very little toxicity *in vivo* and eventually cleared from the body.[201,202] Since incorporating carbon-based conductive materials into bone tissue engineering scaffolds is primarily for implants, they are less likely to enter the bloodstream and translocate to other organs.[203,204] Usui *et al.*[205] investigated the effects of pure MWCNTs, with an average diameter of 80 nm and a length from 10 to 20 μm, in mouse skull and tibial defects to assess their compatibility and influence on bone healing.[205] The results showed that MWCNTs caused a reduced local inflammatory reaction, possessed high bone tissue compatibility and were able to integrate into new bone tissue formation.[205]

Although *in vitro* and *in vivo* research have shown that developing bone scaffolds with CNTs or graphene-based materials has positively influenced cell proliferation, mineralization and bone regeneration with minimal toxicological effects and inflammation,[96,106,203,206] further investigations are still required to better understand their impact on the human body and whether they can be degraded or migrated for their excretion through the kidney and bile ducts for their future use in clinical translation for bone tissue engineering solutions.

6. Conclusions

This review highlights the advantages of incorporating carbon-based conductive materials into a tissue engineering bone scaffold to create a more suitable alternative. Incorporating a carbon-based conductive material directly with an implantable bone scaffold increases protein adsorption promoting bone formation as it facilitates the delivery of electrical stimulation to accelerate cell growth and osteogenic maturation, thus allowing interaction with cell-binding proteins to obtain a fully remodeled bone while conferring mechanical strength. Although there are still concerns associated with the cellular uptake and degradation of carbon-based conductive materials in the human body, the benefits of using an electrically conductive carbon-based component in a bone scaffold may outweigh the disadvantages in most *in vitro* and *in vivo* studies. However, further research associated with the toxicological effects, material migration and excretion of carbon-based conductive materials in bone cells and bone defects within the human body is required. The development of an electrically conductive bone scaffold is proposed as a promising biomaterial for bone tissue engineering solutions capable of supporting cellular bioactivity, withstanding load, and enhancing bone formation and maturation through the application of electrical stimulation to overcome the limitations of the current treatments of bone defects and extend their applications for clinical translation.

Conflicts of interest

There are no conflicts to declare.

Acknowledgements

This work was supported by financial support from the Natural Sciences and Engineering Research Council (NSERC) of Canada.

References

1 R. Burge, B. Dawson-Hughes, D. H. Solomon, J. B. Wong, A. King and A. Tosteson, Incidence and economic burden of osteoporosis-related fractures in the United States, 2005–2025, *J. Bone Miner. Res.*, 2007, **22**, 465–475, DOI: 10.1359/jbmr.061113.

2 J.-E. Tarride, R. B. Hopkins, W. D. Leslie, S. Morin, J. D. Adachi, A. Papaioannou, L. Bessette, J. P. Brown and R. Goeree, The burden of illness of osteoporosis in Canada, *Osteoporosis Int.*, 2012, **23**, 2591–2600, DOI: 10.1007/s00198-012-1931-z.

3 R. B. Hopkins, N. Burke, C. Von Keyserlingk, W. D. Leslie, S. N. Morin, J. D. Adachi, A. Papaioannou, L. Bessette, J. P. Brown, L. Pericleous and J. Tarride, The current economic burden of illness of osteoporosis in Canada, *Osteoporosis Int.*, 2016, **27**, 3023–3032, DOI: 10.1007/s00198-016-3631-6.

4 T.-M. De Witte, L. E. Fratila-Apachitei, A. A. Zadpoor and N. A. Peppas, Bone tissue engineering via growth factor delivery: From scaffolds to complex matrices, *Regener. Biomater.*, 2018, **5**, 197–211, DOI: 10.1093/rb/rby013.

5 A. Wiese and H. C. Pape, Bone defects caused by high-energy injuries, bone loss, infected nonunions, and nonunions, *Orthop. Clin. North Am.*, 2010, **41**, 1–4, DOI: 10.1016/j.ocl.2009.07.003.

6 J.-H. Zeng, S.-W. Liu, L. Xiong, P. Qiu, L.-H. Ding, S.-L. Xiong, J.-T. Li, X.-G. Liao and Z.-M. Tang, Scaffolds for the repair of bone defects in clinical studies: A systematic review, *J. Orthop. Surg.*, 2018, **13**, 33, DOI: 10.1186/s13018-018-0724-2.

7 L. L. Hench, Biomaterials, *Science*, 1980, **208**, 826–831, DOI: 10.1126/science.6246576.

8 R. Arambula-Maldonado, A. Geraili, M. Xing and K. Mequanint, Tissue engineering and regenerative therapeutics: The nexus of chemical engineering and translational medicine, *Can. J. Chem. Eng.*, 2021, cjce.24094, DOI: 10.1002/cjce.24094.

9 L. L. Hench, Bioceramics: From concept to clinic, *J. Am. Ceram. Soc.*, 1991, **74**, 1487–1510, DOI: 10.1111/j.1151-2916.1991.tb07132.x.

10 Q. Fu, M. N. Rahaman, B. S. Bal and R. F. Brown, Preparation and *in vitro* evaluation of bioactive glass (13–93) scaffolds with oriented microstructures for repair and regeneration of load-bearing bones: Preparation and *in vitro* evaluation of bioactive glass scaffolds, *J. Biomed. Mater. Res., Part A*, 2010, **93**, 1380–1390, DOI: 10.1002/jbm.a.32637.

11 B. A. Allo, A. S. Rizkalla and K. Mequanint, Hydroxyapatite formation on sol–gel derived poly(ε-caprolactone)/bioactive glass hybrid biomaterials, *ACS Appl. Mater. Interfaces*, 2012, **4**, 3148–3156, DOI: 10.1021/am300487c.

12 B. A. Allo, S. Lin, K. Mequanint and A. S. Rizkalla, Role of bioactive 3D hybrid fibrous scaffolds on mechanical behavior and spatiotemporal osteoblast gene expression, *ACS Appl. Mater. Interfaces*, 2013, **5**, 7574–7583, DOI: **10.1021/am401861w**.

13 D. Mondal, S. Lin, A. S. Rizkalla and K. Mequanint, Porous and biodegradable polycaprolactone-borophosphosilicate hybrid scaffolds for osteoblast infiltration and stem cell differentiation, *J. Mech. Behav. Biomed. Mater.*, 2019, **92**, 162–171, DOI: **10.1016/j.jmbbm.2019.01.011**.

14 D. Mondal, S. J. Dixon, K. Mequanint and A. S. Rizkalla, Mechanically-competent and cytocompatible polycaprolactone-borophosphosilicate hybrid biomaterials, *J. Mech. Behav. Biomed. Mater.*, 2017, **75**, 180–189, DOI: **10.1016/j.jmbbm.2017.07.010**.

15 N. Aslankoohi, D. Mondal, A. S. Rizkalla and K. Mequanint, Bone repair and regenerative biomaterials: Towards recapitulating the microenvironment, *Polymers*, 2019, **11**, 1437, DOI: **10.3390/polym11091437**.

16 A. G. Guex, J. L. Puetzer, A. Armgarth, E. Littmann, E. Stavrinidou, E. P. Giannelis, G. G. Malliaras and M. M. Stevens, Highly porous scaffolds of PEDOT:PSS for bone tissue engineering, *Acta Biomater.*, 2017, **62**, 91–101, DOI: **10.1016/j.actbio.2017.08.045**.

17 S. Shokri, B. Movahedi, M. Rafieinia and H. Salehi, A new approach to fabrication of Cs/BG/CNT nanocomposite scaffold towards bone tissue engineering and evaluation of its properties, *Appl. Surf. Sci.*, 2015, **357**, 1758–1764, DOI: **10.1016/j.apsusc.2015.10.048**.

18 J. H. Lee, Y. C. Shin, S.-M. Lee, O. S. Jin, S. H. Kang, S. W. Hong, C.-M. Jeong, J. B. Huh and D.-W. Han, Enhanced osteogenesis by reduced graphene oxide/hydroxyapatite nanocomposites, *Sci. Rep.*, 2015, **5**, 18833, DOI: **10.1038/srep18833**.

19 N. Aslankoohi and K. Mequanint, Intrinsically fluorescent bioactive glass-poly(ester amide) hybrid microparticles for dual drug delivery and bone repair, *Mater. Sci. Eng., C*, 2021, **128**, 112288, DOI: **10.1016/j.msec.2021.112288**.

20 E. Fukada and I. Yasuda, On the piezoelectric effect of bone, *J. Phys. Soc. Jpn.*, 1957, **12**, 1158–1162, DOI: **10.1143/JPSJ.12.1158**.

21 The classic: Fundamental aspects of fracture treatment by Iwao Yasuda, reprinted from J. Kyoto Med. Soc., 4, 395–406, 1953, Clin. Orthop. (1977) 5–8.

22 T. W. Balmer, S. Vesztergom, P. Broekmann, A. Stahel and P. Büchler, Characterization of the electrical conductivity of bone and its correlation to osseous structure, *Sci. Rep.*, 2018, **8**, 8601, DOI: **10.1038/s41598-018-26836-0**.

23 A. Saberi, F. Jabbari, P. Zarrintaj, M. R. Saeb and M. Mozafari, Electrically conductive materials: Opportunities and challenges in tissue engineering, *Biomolecules*, 2019, **9**, 448, DOI: **10.3390/biom9090448**.

24 A. Mousavi, S. Vahdat, N. Baheiraei, M. Razavi, M. H. Norahan and H. Baharvand, Multifunctional conductive biomaterials as promising platforms for cardiac tissue engineering, *ACS Biomater. Sci. Eng.*, 2021, **7**, 55–82, DOI: **10.1021/acsbiomaterials.0c01422**.

25 R. Dong, P. X. Ma and B. Guo, Conductive biomaterials for muscle tissue engineering, *Biomaterials*, 2020, **229**, 119584, DOI: **10.1016/j.biomaterials.2019.119584**.

26 P. Zarrintaj, E. Zangene, S. Manouchehri, L. M. Amirabad, N. Baheiraei, M. R. Hadjighasem, M. Farokhi, M. R. Ganjali, B. W. Walker, M. R. Saeb, M. Mozafari, S. Thomas and N. Annabi, Conductive biomaterials as nerve conduits: Recent advances and future challenges, *Appl. Mater. Today*, 2020, **20**, 100784, DOI: **10.1016/j.apmt.2020.100784**.

27 B. Tandon, J. J. Blaker and S. H. Cartmell, Piezoelectric materials as stimulatory biomedical materials and scaffolds for bone repair, *Acta Biomater.*, 2018, **73**, 1–20, DOI: **10.1016/j.actbio.2018.04.026**.

28 C. T. Brighton, W. Wang, R. Seldes, G. Zhang and S. R. Pollack, Signal transduction in electrically stimulated bone cells, *J. Bone Jt. Surg., Am.*, 2001, **83**, 1514–1523, DOI: **10.2106/00004623-200110000-00009**.

29 M. Cerrolaza, V. Duarte and D. Garzón-Alvarado, Analysis of bone remodeling under piezoelectricity effects using boundary elements, *J. Bionic Eng.*, 2017, **14**, 659–671, DOI: **10.1016/S1672-6529(16)60432-8**.

30 R. L. Duncan and C. H. Turner, Mechanotransduction and the functional response of bone to mechanical strain, *Calcif. Tissue Int.*, 1995, **57**, 344–358, DOI: **10.1007/BF00302070**.

31 D. Lilly-Masuda and S. Towne, Bioelectricity and bone healing, *J. Orthop. Sports Phys. Ther.*, 1985, **7**, 54–58, DOI: **10.2519/jospt.1985.7.2.54**.

32 R. B. Heppenstall, Constant direct-current treatment for established nonunion of the Tibia, *Clin. Orthop. NA*, 1983, **179**, 184, DOI: **10.1097/00003086-198309000-00020**.

33 C. T. Brighton, Treatment of nonunion of the Tibia with constant direct current (1980 Fitts Lecture, A.A.S.T.), *J. Trauma: Inj., Infect., Crit. Care*, 1981, **21**, 189–195, DOI: **10.1097/00005373-198103000-00001**.

34 I. S. Aleem, I. Aleem, N. Evaniew, J. W. Busse, M. Yaszemski, A. Agarwal, T. Einhorn and M. Bhandari, Efficacy of electrical stimulators for bone healing: A meta-analysis of randomized Sham-controlled trials, *Sci. Rep.*, 2016, **6**, 31724, DOI: **10.1038/srep31724**.

35 C. A. Bassett, S. N. Mitchell and S. R. Gaston, Treatment of ununited tibial diaphyseal fractures with pulsing electromagnetic fields, *J. Bone Jt. Surg.*, 1981, **63**, 511–523, DOI: **10.2106/00004623-198163040-00001**.

36 M. B. Bhavsar, L. Leppik, K. M.-C. Oliveira and J. H. Barker, Electrical stimulation–fracture treatment: New insights into the underlying mechanisms, *Bioelectron. Med.*, 2019, **2**, 5–7, DOI: **10.2217/bem-2019-0010**.

37 W. Sharrard, A double-blind trial of pulsed electromagnetic fields for delayed union of tibial fractures, *J. Bone Joint Surg. Br.*, 1990, **72-B**, 347–355, DOI: **10.1302/0301-620X.72B3.2187877**.

38 O. Wahlström, Stimulation of fracture healing with electromagnetic fields of extremely low frequency (EMF of ELF), *Clin. Orthop.*, 1984, 293–301.

39 H. Shi, J. Xiong, Y. Chen, J. Wang, X. Qiu, Y. Wang and Y. Qiu, Early application of pulsed electromagnetic field in the treatment of postoperative delayed union of long-bone fractures: A prospective randomized controlled study, *BMC Musculoskeletal Disord.*, 2013, **14**, 35, DOI: **10.1186/1471-2474-14-35**.

40 G. Borsalino, M. Bagnacani, E. Bettati, F. Fornaciari, R. Rocchi, S. Uluhogian, G. Ceccherelli, R. Cadossi and G. C. Traina, Electrical stimulation of human femoral intertrochanteric osteotomies: Double-blind study, *Clin. Orthop. NA*, 1988, 256–263, DOI: **10.1097/00003086-198812000-00037**.

41 X. Tian, X. Li, L. Zhou, J. Zhao, X. Li, Y. Huang and T. Ding, On the effect of electroacupuncture in promoting healing after high Tibial osteotomy, *Comput. Math. Methods Med.*, 2022, **2022**, 1–7, DOI: **10.1155/2022/6428759**.

42 C. A.-L. Bassett and M. M. Schink, Treatment of therapeutically resistant non-unions with bone grafts and pulsing electromagnetic fields, *J. Bone Jt. Surg., Am. Vol.*, 1982, **64**, 1214–1220.

43 L. Leppik, K. M.-C. Oliveira, M. B. Bhavsar and J. H. Barker, Electrical stimulation in bone tissue engineering treatments, *Eur. J. Trauma Emerg. Surg.*, 2020, **46**, 231–244, DOI: **10.1007/s00068-020-01324-1**.

44 P. J. Nicksic, D. T. Donnelly, M. Hesse, S. Bedi, N. Verma, A. J. Seitz, A. J. Shoffstall, K. A. Ludwig, A. M. Dingle and S. O. Poore, Electronic Bone Growth Stimulators for Augmentation of Osteogenesis in In Vitro and In Vivo Models: A Narrative Review of Electrical Stimulation Mechanisms and Device Specifications, *Front. Bioeng. Biotechnol.*, 2022, **10**, 793945, DOI: **10.3389/fbioe.2022.793945**.

45 M. E. Steinberg, C. T. Brighton, A. Corces, G. D. Hayken, D. R. Steinberg, B. Strafford, S. E. Tooze and M. Fallon, Osteonecrosis of the femoral head. Results of core decompression and grafting with and without electrical stimulation, *Clin. Orthop.*, 1989, 199–208.

46 S. Fornell, J. Ribera, M. Mella, A. Carranza, D. Serrano-Toledano and G. Domecq, Effects of electrical stimulation in the treatment of osteonecrosis of the femoral head, *HIP Int.*, 2018, **28**, 434–441, DOI: **10.5301/hipint.5000581**.

47 C. T. Brighton, Z. B. Friedenberg, E. I. Mitchell and R. E. Booth, Treatment of nonunion with constant direct current, *Clin. Orthop.*, 1977, 106–123.

48 R. O. Becker, J. A. Spadaro and A. A. Marino, Clinical experiences with low intensity direct current stimulation of bone growth, *Clin. Orthop.*, 1977, 75–83.

49 J. C. Gan, D. C. Fredericks and P. A. Glazer, Direct current and capacitive coupling electrical stimulation upregulates osteopromotive factors for spinal fusions, (n.d.) 4.

50 F. Benazzo, M. Mosconi, G. Beccarisi and U. Galli, Use of Capacitive Coupled Electric Fields in Stress Fractures in Athletes:, *Clin. Orthop. NA*, 1995, **145–**, 149, DOI: **10.1097/00003086-199501000-00023**.

51 W. Li, W. Liu, W. Wang, J. Wang, T. Ma, J. Chen, H. Wu and C. Liu, Sinusoidal electromagnetic fields accelerate bone regeneration by boosting the multifunctionality of bone marrow mesenchymal stem cells, *Stem Cell Res. Ther.*, 2021, **12**, 234, DOI: **10.1186/s13287-021-02302-z**.

52 L. Peng, C. Fu, F. Xiong, Q. Zhang, Z. Liang, L. Chen, C. He and Q. Wei, Effectiveness of pulsed electromagnetic fields on bone healing: A systematic review and meta-analysis of randomized controlled trials, *Bioelectromagnetics*, 2020, **41**, 323–337, DOI: **10.1002/bem.22271**.

53 P. F.-W. Hannemann, E. H.-H. Mommers, J. P.-M. Schots, P. R.-G. Brink and M. Poeze, The effects of low-intensity pulsed ultrasound and pulsed electromagnetic fields bone growth stimulation in acute fractures: A systematic review and meta-analysis of randomized controlled trials, *Arch. Orthop. Trauma Surg.*, 2014, **134**, 1093–1106, DOI: **10.1007/s00402-014-2014-8**.

54 X. Zhang, J. Zhang, X. Qu and J. Wen, Effects of different extremely low-frequency electromagnetic fields on osteoblasts, *Electromagn. Biol. Med.*, 2007, **26**, 167–177, DOI: **10.1080/15368370701580756**.

55 H. Murray and B. Pethica, A follow-up study of the in-practice results of pulsed electromagnetic field therapy in the management of nonunion fractures, *Orthop. Res. Rev.*, 2016, **8**, 67–72, DOI: **10.2147/ORR.S113756**.

56 A. M. Hollenberg, A. Huber, C. O. Smith and R. A. Eliseev, Electromagnetic stimulation increases mitochondrial function in osteogenic cells and promotes bone fracture repair, *Sci. Rep.*, 2021, **11**, 19114, DOI: **10.1038/s41598-021-98625-1**.

57 EBI bone healing system, *Case Manager*, 1999, **10**, 37–40, DOI: **10.1016/S1061-9259(99)80129-5**.

58 S. Akhter, A. R. Qureshi, I. Aleem, H. A. El-Khechen, S. Khan, O. Sikder, M. Khan, M. Bhandari and I. Aleem, Efficacy of electrical stimulation for spinal fusion: A systematic review and meta-analysis of randomized controlled trials, *Sci. Rep.*, 2020, **10**, 4568, DOI: **10.1038/s41598-020-61266-x**.

59 E. Kozhevnikov, X. Hou, S. Qiao, Y. Zhao, C. Li and W. Tian, Electrical impedance spectroscopy – A potential method for the study and monitoring of a bone critical-size defect healing process treated with bone tissue engineering and regenerative medicine approaches, *J. Mater. Chem. B*, 2016, **4**, 2757–2767, DOI: **10.1039/C5TB02707A**.

60 C. Bonifasi-Lista and E. Cherkaev, Electrical impedance spectroscopy as a potential tool for recovering bone porosity, *Phys. Med. Biol.*, 2009, **54**, 3063–3082, DOI: **10.1088/0031-9155/54/10/007**.

61 B. Guo and P. X. Ma, Conducting polymers for tissue engineering, *Biomacromolecules*, 2018, **19**, 1764–1782, DOI: **10.1021/acs.biomac.8b00276**.

62 S. Goodarzi, T. Da Ros, J. Conde, F. Sefat and M. Mozafari, Fullerene: Biomedical engineers get to revisit an old friend, *Mater. Today*, 2017, **20**, 460–480, DOI: **10.1016/j.mattod.2017.03.017**.

63 S. Ahadian, R. Obregón, J. Ramón-Azcón, G. Salazar, H. Shiku, M. Ramalingam and T. Matsue, Carbon nanotubes and graphene-based nanomaterials for stem cell differentiation and tissue regeneration, *J. Nanosci.*

Nanotechnol., 2016, **16**, 8862–8880, DOI: 10.1166/jnn.2016.12729.

64 B. Ribeiro, E. C. Botelho, M. L. Costa and C. F. Bandeira, Carbon nanotube buckypaper reinforced polymer composites: A review, *Polímeros*, 2017, **27**, 247–255, DOI: 10.1590/0104-1428.03916.

65 Y. Liu, M. Park, H. K. Shin, B. Pant, J. Choi, Y. W. Park, J. Y. Lee, S.-J. Park and H.-Y. Kim, Facile preparation and characterization of poly(vinyl alcohol)/chitosan/graphene oxide biocomposite nanofibers, *J. Ind. Eng. Chem.*, 2014, **20**, 4415–4420, DOI: 10.1016/j.jiec.2014.02.009.

66 Y. Zhu, S. Murali, W. Cai, X. Li, J. W. Suk, J. R. Potts and R. S. Ruoff, Graphene and graphene oxide: Synthesis, properties, and applications, *Adv. Mater.*, 2010, **22**, 3906–3924, DOI: 10.1002/adma.201001068.

67 M. J. Green, N. Behabtu, M. Pasquali and W. W. Adams, Nanotubes as polymers, *Polymer.*, 2009, **50**, 4979–4997, DOI: 10.1016/j.polymer.2009.07.044.

68 H. W. Kroto, J. R. Heath, S. C. O'Brien, R. F. Curl and R. E. Smalley, C60: Buckminsterfullerene, *Nature*, 1985, **318**, 162–163, DOI: 10.1038/318162a0.

69 T. Guo, P. Nikolaev, A. Thess, D. T. Colbert and R. E. Smalley, Catalytic growth of single-walled nanotubes by laser vaporization, *Chem. Phys. Lett.*, 1995, **243**, 49–54, DOI: 10.1016/0009-2614(95)00825-O.

70 A. Thess, R. Lee, P. Nikolaev, H. Dai, P. Petit, J. Robert, C. Xu, Y. H. Lee, S. G. Kim, A. G. Rinzler, D. T. Colbert, G. E. Scuseria, D. Tománek, J. E. Fischer and R. E. Smalley, Crystalline ropes of metallic carbon nanotubes, *Science*, 1996, **273**, 483–487, DOI: 10.1126/science.273.5274.483.

71 A. Eatemadi, H. Daraee, H. Karimkhanloo, M. Kouhi, N. Zarghami, A. Akbarzadeh, M. Abasi, Y. Hanifehpour and S. W. Joo, Carbon nanotubes: properties, synthesis, purification, and medical applications, *Nanoscale Res. Lett.*, 2014, **9**, 393, DOI: 10.1186/1556-276X-9-393.

72 S. Iijima, Helical microtubules of graphitic carbon, *Nature*, 1991, **354**, 56–58, DOI: 10.1038/354056a0.

73 T. W. Ebbesen and P. M. Ajayan, Large-scale synthesis of carbon nanotubes, *Nature*, 1992, **358**, 220–222, DOI: 10.1038/358220a0.

74 D. S. Bethune, C. H. Kiang, M. S. de Vries, G. Gorman, R. Savoy, J. Vazquez and R. Beyers, Cobalt-catalysed growth of carbon nanotubes with single-atomic-layer walls, *Nature*, 1993, **363**, 605–607, DOI: 10.1038/363605a0.

75 D. Chauhan, A. Pujari, G. Zhang, K. Dasgupta, V. N. Shanov and M. J. Schulz, Effect of a metallocene catalyst mixture on CNT yield using the FC-CVD process, *Catalysts*, 2022, **12**, 287, DOI: 10.3390/catal12030287.

76 A. Yahyazadeh and B. Khoshandam, Carbon nanotube synthesis via the catalytic chemical vapor deposition of methane in the presence of iron, molybdenum, and iron–molybdenum alloy thin layer catalysts, *Res. Phys.*, 2017, **7**, 3826–3837, DOI: 10.1016/j.rinp.2017.10.001.

77 Y. Yan, F. Z. Nashath, S. Chen, S. Manickam, S. S. Lim, H. Zhao, E. Lester, T. Wu and C. H. Pang, Synthesis of graphene: Potential carbon precursors and approaches, *Nanotechnol. Rev.*, 2020, **9**, 1284–1314, DOI: 10.1515/ntrev-2020-0100.

78 J. Dong, L. Zhang, X. Dai and F. Ding, The epitaxy of 2D materials growth, *Nat. Commun.*, 2020, **11**, 5862, DOI: 10.1038/s41467-020-19752-3.

79 N. Hong, W. Yang, C. Bao, S. Jiang, L. Song and Y. Hu, Facile synthesis of graphene by pyrolysis of poly(methyl methacrylate) on nickel particles in the confined microzones, *Mater. Res. Bull.*, 2012, **47**, 4082–4088, DOI: 10.1016/j.materresbull.2012.08.049.

80 X. Kong, Y. Zhu, H. Lei, C. Wang, Y. Zhao, E. Huo, X. Lin, Q. Zhang, M. Qian, W. Mateo, R. Zou, Z. Fang and R. Ruan, Synthesis of graphene-like carbon from biomass pyrolysis and its applications, *Chem. Eng. J.*, 2020, **399**, 125808, DOI: 10.1016/j.cej.2020.125808.

81 A. Yakubu, Graphene synthesis by chemical vapour deposition (CVD): A review on growth mechanism and techniques, *Int. J. Eng. Res.*, 2019, **8**, IJERTV8IS050012, DOI: 10.17577/IJERTV8IS050012.

82 K. S. Novoselov, Electric field effect in atomically thin carbon films, *Science*, 2004, **306**, 666–669, DOI: 10.1126/science.1102896.

83 E. Andrijanto, S. Shoelarta, G. Subiyanto and S. Rifki, *Facile synthesis of graphene from graphite using ascorbic acid as reducing agent*, Semarang, Indonesia, 2016, p. 020003, DOI: 10.1063/1.4945457.

84 W. S. Hummers and R. E. Offeman, Preparation of graphitic oxide, *J. Am. Chem. Soc.*, 1958, **80**, 1339, DOI: 10.1021/ja01539a017.

85 G. Shao, Y. Lu, F. Wu, C. Yang, F. Zeng and Q. Wu, Graphene oxide: The mechanisms of oxidation and exfoliation, *J. Mater. Sci.*, 2012, **47**, 4400–4409, DOI: 10.1007/s10853-012-6294-5.

86 N. Kumar and V. C. Srivastava, Simple synthesis of large graphene oxide sheets *via* electrochemical method coupled with oxidation process, *ACS Omega*, 2018, **3**, 10233–10242, DOI: 10.1021/acsomega.8b01283.

87 D. Roy Chowdhury, C. Singh and A. Paul, Role of graphite precursor and sodium nitrate in graphite oxide synthesis, *RSC Adv.*, 2014, **4**, 15138, DOI: 10.1039/c4ra01019a.

88 S. Pei and H.-M. Cheng, The reduction of graphene oxide, *Carbon*, 2012, **50**, 3210–3228, DOI: 10.1016/j.carbon.2011.11.010.

89 X. Yang, E. Li, Y. Wan, P. Smith, G. Shang and Q. Cui, Antioxidative fullerol promotes osteogenesis of human adipose-derived stem cells, *Int. J. Nanomed.*, 2014, 4023, DOI: 10.2147/IJN.S66785.

90 P. Piotrowski, K. Klimek, G. Ginalska and A. Kaim, Beneficial influence of water-soluble PEG-functionalized C60 fullerene on human osteoblast growth in vitro, *Materials*, 2021, **14**, 1566, DOI: 10.3390/ma14061566.

91 V. Krishnan, Y. Kasuya, Q. Ji, M. Sathish, L. K. Shrestha, S. Ishihara, K. Minami, H. Morita, T. Yamazaki, N. Hanagata, K. Miyazawa, S. Acharya, W. Nakanishi, J. P. Hill and K. Ariga, Vortex-aligned fullerene nanowhiskers as a scaffold for orienting cell growth, *ACS Appl. Mater.*

Interfaces, 2015, **7**, 15667–15673, DOI: 10.1021/acsami.5b04811.

92 J. Yang, J. Liang, Y. Zhu, M. Hu, L. Deng, W. Cui and X. Xu, Fullerol-hydrogel microfluidic spheres for in situ redox regulation of stem cell fate and refractory bone healing, *Bioact. Mater.*, 2021, **6**, 4801–4815, DOI: 10.1016/j.bioactmat.2021.05.024.

93 S. Constanda, M. S. Stan, C. S. Ciobanu, M. Motelica-Heino, R. Guégan, K. Lafdi, A. Dinischiotu and D. Predoi, Carbon nanotubes-hydroxyapatite nanocomposites for an improved osteoblast cell response, *J. Nanomater.*, 2016, 1–10, DOI: 10.1155/2016/3941501.

94 X. Liu, M. N. George, S. Park, A. L. Miller II, B. Gaihre, L. Li, B. E. Waletzki, A. Terzic, M. J. Yaszemski and L. Lu, 3D-printed scaffolds with carbon nanotubes for bone tissue engineering: Fast and homogeneous one-step functionalization, *Acta Biomater.*, 2020, **111**, 129–140, DOI: 10.1016/j.actbio.2020.04.047.

95 S. Qian, Z. Yan, Y. Xu, H. Tan, Y. Chen, Z. Ling and X. Niu, Carbon nanotubes as electrophysiological building blocks for a bioactive cell scaffold through biological assembly to induce osteogenesis, *RSC Adv.*, 2019, **9**, 12001–12009, DOI: 10.1039/C9RA00370C.

96 X. Li, H. Liu, X. Niu, B. Yu, Y. Fan, Q. Feng, F. Cui and F. Watari, The use of carbon nanotubes to induce osteogenic differentiation of human adipose-derived MSCs *in vitro* and ectopic bone formation *in vivo*, *Biomaterials*, 2012, **33**, 4818–4827, DOI: 10.1016/j.biomaterials.2012.03.045.

97 K. Dixit and N. Sinha, Additive manufacturing of carbon nanotube reinforced bioactive glass scaffolds for bone tissue engineering, *J. Eng. Sci. Med. Diagn. Ther.*, 2021, **4**, 041004, DOI: 10.1115/1.4051801.

98 A. G. Sanchez, E. Prokhorov, G. Luna-Barcenas, J. Hernández-Vargas, R. Román-Doval, S. Mendoza and H. Rojas-Chávez, Chitosan-hydroxyapatite-MWCNTs nanocomposite patch for bone tissue engineering applications, *Mater. Today Commun.*, 2021, **28**, 102615, DOI: 10.1016/j.mtcomm.2021.102615.

99 E. P.-e Silva, B. Huang, J. V. Helaehil, P. R.-L. Nalesso, L. Bagne, M. A. de Oliveira, G. C.-C. Albiazetti, A. Aldalbahi, M. El-Newehy, M. Santamaria-Jr, F. A.-S. Mendonça, P. Bártolo and G. F. Caetano, In vivo study of conductive 3D printed PCL/MWCNTs scaffolds with electrical stimulation for bone tissue engineering, *Bio-Des. Manuf.*, 2021, **4**, 190–202, DOI: 10.1007/s42242-020-00116-1.

100 W. Lan, X. Zhang, M. Xu, L. Zhao, D. Huang, X. Wei and W. Chen, Carbon nanotube reinforced polyvinyl alcohol/biphasic calcium phosphate scaffold for bone tissue engineering, *RSC Adv.*, 2019, **9**, 38998–39010, DOI: 10.1039/C9RA08569F.

101 L. Liu, B. Yang, L.-Q. Wang, J.-P. Huang, W.-Y. Chen, Q. Ban, Y. Zhang, R. You, L. Yin and Y.-Q. Guan, Biomimetic bone tissue engineering hydrogel scaffolds constructed using ordered CNTs and HA induce the proliferation and differentiation of BMSCs, *J. Mater. Chem. B*, 2020, **8**, 558–567, DOI: 10.1039/C9TB01804B.

102 A. Rajan Unnithan, A. Ramachandra Kurup Sasikala, C. H. Park and C. S. Kim, A unique scaffold for bone tissue engineering: An osteogenic combination of graphene oxide–hyaluronic acid–chitosan with simvastatin, *J. Ind. Eng. Chem.*, 2017, **46**, 182–191, DOI: 10.1016/j.jiec.2016.10.029.

103 S. Bahrami, N. Baheiraei and M. Shahrezaee, Biomimetic reduced graphene oxide coated collagen scaffold for in situ bone regeneration, *Sci. Rep.*, 2021, **11**, 16783, DOI: 10.1038/s41598-021-96271-1.

104 J. Lu, C. Cheng, Y.-S. He, C. Lyu, Y. Wang, J. Yu, L. Qiu, D. Zou and D. Li, Multilayered Graphene Hydrogel Membranes for Guided Bone Regeneration, *Adv. Mater.*, 2016, **28**, 4025–4031, DOI: 10.1002/adma.201505375.

105 Y. Li, J. He, J. Zhou, Z. Li, L. Liu, S. Hu, B. Guo and W. Wang, A conductive photothermal non-swelling nanocomposite hydrogel patch accelerating bone defect repair, *Biomater. Sci.*, 2022, **10**, 1326–1341, DOI: 10.1039/D1BM01937F.

106 H. Fang, C. Luo, S. Liu, M. Zhou, Y. Zeng, J. Hou, L. Chen, S. Mou, J. Sun and Z. Wang, A biocompatible vascularized graphene oxide (GO)-collagen chamber with osteoinductive and anti-fibrosis effects promotes bone regeneration *in vivo*, *Theranostics*, 2020, **10**, 2759–2772, DOI: 10.7150/thno.42006.

107 J. Sun, L. Li, F. Xing, Y. Yang, M. Gong, G. Liu, S. Wu, R. Luo, X. Duan, M. Liu, M. Zou and Z. Xiang, Graphene oxide-modified silk fibroin/nanohydroxyapatite scaffold loaded with urine-derived stem cells for immunomodulation and bone regeneration, *Stem Cell Res. Ther.*, 2021, **12**, 591, DOI: 10.1186/s13287-021-02634-w.

108 H. Belaid, S. Nagarajan, C. Teyssier, C. Barou, J. Barés, S. Balme, H. Garay, V. Huon, D. Cornu, V. Cavaillès and M. Bechelany, Development of new biocompatible 3D printed graphene oxide-based scaffolds, *Mater. Sci. Eng. C.*, 2020, **110**, 110595, DOI: 10.1016/j.msec.2019.110595.

109 X. Xie, K. Hu, D. Fang, L. Shang, S. D. Tran and M. Cerruti, Graphene and hydroxyapatite self-assemble into homogeneous, free standing nanocomposite hydrogels for bone tissue engineering, *Nanoscale*, 2015, **7**, 7992–8002, DOI: 10.1039/C5NR01107H.

110 M. H. Norahan, M. Amroon, R. Ghahremanzadeh, N. Rabiee and N. Baheiraei, Reduced graphene oxide: Osteogenic potential for bone tissue engineering, *IET Nanobiotechnol.*, 2019, **13**, 720–725, DOI: 10.1049/iet-nbt.2019.0125.

111 M. S. Kang, S. J. Jeong, S. H. Lee, B. Kim, S. W. Hong, J. H. Lee and D.-W. Han, Reduced graphene oxide coating enhances osteogenic differentiation of human mesenchymal stem cells on Ti surfaces, *Biomater. Res.*, 2021, **25**, 4, DOI: 10.1186/s40824-021-00205-x.

112 H. Golzar, D. Mohammadrezaei, A. Yadegari, M. Rasoulianboroujeni, M. Hashemi, M. Omidi, F. Yazdian, M. Shalbaf and L. Tayebi, Incorporation of functionalized reduced graphene oxide/magnesium nanohybrid to enhance the osteoinductivity capability of 3D printed calcium

phosphate-based scaffolds, *Composites, Part B*, 2020, **185**, 107749, DOI: 10.1016/j.compositesb.2020.107749.

113 W. Wu, W. Chen, D. Lin and K. Yang, Influence of surface oxidation of multiwalled carbon nanotubes on the adsorption affinity and capacity of polar and nonpolar organic compounds in aqueous phase, *Environ. Sci. Technol.*, 2012, **46**, 5446–5454, DOI: 10.1021/es3004848.

114 M. Simsikova and T. Sikola, Interaction of graphene oxide with proteins and applications of their conjugates, *J. Nanomed. Res.*, 2017, **5**, 00109, DOI: 10.15406/jnmr.2017.05.00109.

115 D. Xiao, W. Sun, H. Dai, Y. Zhang, X. Qin, L. Li, Z. Wei and X. Chen, Influence of charge states on the π–π interactions of aromatic side chains with surface of graphene sheet and single-walled carbon nanotubes in bioelectrodes, *J. Phys. Chem. C*, 2014, **118**, 20694–20701, DOI: 10.1021/jp506336c.

116 D. Li, W. Zhang, X. Yu, Z. Wang, Z. Su and G. Wei, When biomolecules meet graphene: From molecular level interactions to material design and applications, *Nanoscale*, 2016, **8**, 19491–19509, DOI: 10.1039/C6NR07249F.

117 P. Hampitak, D. Melendrez, M. Iliut, M. Fresquet, N. Parsons, B. Spencer, T. A. Jowitt and A. Vijayaraghavan, Protein interactions and conformations on graphene-based materials mapped using a quartz-crystal microbalance with dissipation monitoring (QCM-D), *Carbon*, 2020, **165**, 317–327, DOI: 10.1016/j.carbon.2020.04.093.

118 S. Namgung, K. Y. Baik, J. Park and S. Hong, Controlling the growth and differentiation of human mesenchymal stem cells by the arrangement of individual carbon nanotubes, *ACS Nano.*, 2011, **5**, 7383–7390, DOI: 10.1021/nn2023057.

119 D. Y. Lee, Z. Khatun, J.-H. Lee, Y. Lee and I. In, Blood compatible graphene/heparin conjugate through noncovalent chemistry, *Biomacromolecules*, 2011, **12**, 336–341, DOI: 10.1021/bm101031a.

120 S. Wang, E. S. Humphreys, S.-Y. Chung, D. F. Delduco, S. R. Lustig, H. Wang, K. N. Parker, N. W. Rizzo, S. Subramoney, Y.-M. Chiang and A. Jagota, Peptides with selective affinity for carbon nanotubes, *Nat. Mater.*, 2003, **2**, 196–200, DOI: 10.1038/nmat833.

121 C. Rajesh, C. Majumder, H. Mizuseki and Y. Kawazoe, A theoretical study on the interaction of aromatic amino acids with graphene and single walled carbon nanotube, *J. Chem. Phys.*, 2009, **130**, 124911, DOI: 10.1063/1.3079096.

122 K. Iwashita, K. Shiraki, R. Ishii, T. Tanaka and A. Hirano, Liquid chromatographic analysis of the interaction between amino acids and aromatic surfaces using single-wall carbon nanotubes, *Langmuir*, 2015, **31**, 8923–8929, DOI: 10.1021/acs.langmuir.5b02500.

123 A. Hirano and T. Kameda, Aromaphilicity index of amino acids: Molecular dynamics simulations of the protein binding affinity for carbon nanomaterials, *ACS Appl. Nano Mater.*, 2021, **4**, 2486–2495, DOI: 10.1021/acsanm.0c03047.

124 Y. Chong, C. Ge, Z. Yang, J. A. Garate, Z. Gu, J. K. Weber, J. Liu and R. Zhou, Reduced cytotoxicity of graphene nanosheets mediated by blood-protein coating, *ACS Nano.*, 2015, **9**, 5713–5724, DOI: 10.1021/nn5066606.

125 M. Taale, F. Schütt, K. Zheng, Y. K. Mishra, A. R. Boccaccini, R. Adelung and C. Selhuber-Unkel, Bioactive carbon-based hybrid 3D scaffolds for osteoblast growth, *ACS Appl. Mater. Interfaces*, 2018, **10**, 43874–43886, DOI: 10.1021/acsami.8b13631.

126 C. Fu, H. Bai, J. Zhu, Z. Niu, Y. Wang, J. Li, X. Yang and Y. Bai, Enhanced cell proliferation and osteogenic differentiation in electrospun PLGA/hydroxyapatite nanofibre scaffolds incorporated with graphene oxide, *PLoS One*, 2017, **12**, e0188352, DOI: 10.1371/journal.pone.0188352.

127 Z. Du, X. Feng, G. Cao, Z. She, R. Tan, K. E. Aifantis, R. Zhang and X. Li, The effect of carbon nanotubes on osteogenic functions of adipose-derived mesenchymal stem cells in vitro and bone formation in vivo compared with that of nano-hydroxyapatite and the possible mechanism, *Bioact. Mater.*, 2021, **6**, 333–345, DOI: 10.1016/j.bioactmat.2020.08.015.

128 H. Cindrič, B. Kos, G. Tedesco, M. Cadossi, A. Gasbarrini and D. Miklavčič, Electrochemotherapy of spinal metastases using transpedicular approach—A numerical feasibility study, *Technol. Cancer Res. Treat.*, 2018, **17**, 153303461877025, DOI: 10.1177/1533034618770253.

129 Electrical Conductivity of Carbon Nanotube and Graphene-Based Nanocomposites, in *Micromechanics and nanomechanics of composite solids*, ed. S. A. Meguid and G. J. Weng, Springer International Publishing, Cham, 2018, DOI: 10.1007/978-3-319-52794-9.

130 G. Yang, L. Li, W. B. Lee and M. C. Ng, Structure of graphene and its disorders: a review, *Sci. Technol. Adv. Mater.*, 2018, **19**, 613–648, DOI: 10.1080/14686996.2018.1494493.

131 Y. Wang and G. J. Weng, Electrical conductivity of carbon nanotube- and graphene-based nanocomposites, in *Micromechanics Nanomechanics Compos. Solids*, ed. S. A. Meguid and G. J. Weng, Springer International Publishing, Cham, 2018, pp. 123–156, DOI: 10.1007/978-3-319-52794-9_4.

132 W. Bauhofer and J. Z. Kovacs, A review and analysis of electrical percolation in carbon nanotube polymer composites, *Compos. Sci. Technol.*, 2009, **69**, 1486–1498, DOI: 10.1016/j.compscitech.2008.06.018.

133 H. Wei, J. Cui, K. Lin, J. Xie and X. Wang, Recent advances in smart stimuli-responsive biomaterials for bone therapeutics and regeneration, *Bone Res.*, 2022, **10**, 17, DOI: 10.1038/s41413-021-00180-y.

134 R. Balint, N. J. Cassidy and S. H. Cartmell, Electrical stimulation: A novel tool for tissue engineering, *Tissue Eng. Part B*, 2013, **19**, 48–57, DOI: 10.1089/ten.teb.2012.0183.

135 M. Griffin and A. Bayat, Electrical stimulation in bone healing: Critical analysis by evaluating levels of evidence, *Eplasty*, 2011, **11**, e34.

136 J. Kuan-Jung Li, J. Cheng-An Lin, H.-C. Liu, J.-S. Sun, R.-C. Ruaan, C. Shih and W. H.-S. Chang, Comparison of ultrasound and electromagnetic field effects on osteoblast growth, *Ultrasound Med. Biol.*, 2006, 769–775, DOI: 10.1016/j.ultrasmedbio.2006.01.017.

137 H. Zhuang, W. Wang, R. M. Seldes, A. D. Tahernia, H. Fan and C. T. Brighton, Electrical stimulation induces the level

of TGF-β1 mRNA in osteoblastic cells by a mechanism involving calcium/calmodulin pathway, *Biochem. Biophys. Res. Commun.*, 1997, **237**, 225–229, DOI: **10.1006/bbrc.1997.7118**.

138 K. Srirussamee, S. Mobini, N. J. Cassidy and S. H. Cartmell, Direct electrical stimulation enhances osteogenesis by inducing Bmp2 and Spp1 expressions from macrophages and preosteoblasts, *Biotechnol. Bioeng.*, 2019, **116**, 3421–3432, DOI: **10.1002/bit.27142**.

139 Y. Huang, W. Jing, Y. Li, Q. Cai and X. Yang, Composites made of polyorganophosphazene and carbon nanotube up-regulating osteogenic activity of BMSCs under electrical stimulation, *Colloids Surf., B*, 2021, **204**, 111785, DOI: **10.1016/j.colsurfb.2021.111785**.

140 D. Jamal and R. C. de Guzman, Silicone substrate with collagen and carbon nanotubes exposed to pulsed current for MSC osteodifferentiation, *Int. J. Biomater.*, 2017, 1–9, DOI: **10.1155/2017/3684812**.

141 J. Cao, Z. Liu, L. Zhang, J. Li, H. Wang and X. Li, Advance of electroconductive hydrogels for biomedical applications in orthopedics, *Adv. Mater. Sci. Eng.*, 2021, 1–13, DOI: **10.1155/2021/6668209**.

142 N. Amiryaghoubi, N. Noroozi Pesyan, M. Fathi and Y. Omidi, Injectable thermosensitive hybrid hydrogel containing graphene oxide and chitosan as dental pulp stem cells scaffold for bone tissue engineering, *Int. J. Biol. Macromol.*, 2020, **162**, 1338–1357, DOI: **10.1016/j.ijbiomac.2020.06.138**.

143 L. Wang, R. Lu, J. Hou, X. Nan, Y. Xia, Y. Guo, K. Meng, C. Xu, X. Wang and B. Zhao, Application of injectable silk fibroin/graphene oxide hydrogel combined with bone marrow mesenchymal stem cells in bone tissue engineering, *Colloids Surf. Physicochem. Eng. Asp.*, 2020, **604**, 125318, DOI: **10.1016/j.colsurfa.2020.125318**.

144 X. Liu, M. N. George, L. Li, D. Gamble, A. L. Miller II, B. Gaihre, B. E. Waletzki and L. Lu, Injectable electrical conductive and phosphate releasing gel with two-dimensional black phosphorus and carbon nanotubes for bone tissue engineering, *ACS Biomater. Sci. Eng.*, 2020, **6**, 4653–4665, DOI: **10.1021/acsbiomaterials.0c00612**.

145 W. Wang, J. R.-P. Junior, P. R.-L. Nalesso, D. Musson, J. Cornish, F. Mendonça, G. F. Caetano and P. Bártolo, Engineered 3D printed poly(ε-caprolactone)/graphene scaffolds for bone tissue engineering, *Mater. Sci. Eng., C*, 2019, **100**, 759–770, DOI: **10.1016/j.msec.2019.03.047**.

146 H. Siddiqui, K. Pickering and M. Mucalo, A review on the use of hydroxyapatite-carbonaceous structure composites in bone replacement materials for strengthening purposes, *Materials*, 2018, **11**, 1813, DOI: **10.3390/ma11101813**.

147 J. W. Suk, R. D. Piner, J. An and R. S. Ruoff, Mechanical properties of monolayer graphene oxide, *ACS Nano*, 2010, **4**, 6557–6564, DOI: **10.1021/nn101781v**.

148 C. Gómez-Navarro, M. Burghard and K. Kern, Elastic properties of chemically derived single graphene sheets, *Nano Lett.*, 2008, **8**, 2045–2049, DOI: **10.1021/nl801384y**.

149 D. G. Papageorgiou, I. A. Kinloch and R. J. Young, Mechanical properties of graphene and graphene-based nanocomposites, *Prog. Mater. Sci.*, 2017, **90**, 75–127, DOI: **10.1016/j.pmatsci.2017.07.004**.

150 M. Tarfaoui, K. Lafdi and A. El Moumen, Mechanical properties of carbon nanotubes based polymer composites, *Composites, Part B*, 2016, **103**, 113–121, DOI: **10.1016/j.compositesb.2016.08.016**.

151 J. Li, Z. Zhang, J. Fu, Z. Liang and K. R. Ramakrishnan, Mechanical properties and structural health monitoring performance of carbon nanotube-modified FRP composites: A review, *Nanotechnol. Rev.*, 2021, **10**, 1438–1468, DOI: **10.1515/ntrev-2021-0104**.

152 A. Takakura, K. Beppu, T. Nishihara, A. Fukui, T. Kozeki, T. Namazu, Y. Miyauchi and K. Itami, Strength of carbon nanotubes depends on their chemical structures, *Nat. Commun.*, 2019, **10**, 3040, DOI: **10.1038/s41467-019-10959-7**.

153 M. G. Pastore Carbone, G. Tsoukleri, A. C. Manikas, E. Makarona, C. Tsamis and C. Galiotis, Production and mechanical characterization of graphene micro-ribbons, *J. Compos. Sci.*, 2019, **3**, 42, DOI: **10.3390/jcs3020042**.

154 M.-F. Yu, B. S. Files, S. Arepalli and R. S. Ruoff, Tensile loading of ropes of single wall carbon nanotubes and their mechanical properties, *Phys. Rev. Lett.*, 2000, **84**, 5552–5555, DOI: **10.1103/PhysRevLett.84.5552**.

155 P. Zhang, L. Ma, F. Fan, Z. Zeng, C. Peng, P. E. Loya, Z. Liu, Y. Gong, J. Zhang, X. Zhang, P. M. Ajayan, T. Zhu and J. Lou, Fracture toughness of graphene, *Nat. Commun.*, 2014, **5**, 3782, DOI: **10.1038/ncomms4782**.

156 M. Zu, W. Lu, Q.-W. Li, Y. Zhu, G. Wang and T.-W. Chou, Characterization of carbon nanotube fiber compressive properties using tensile recoil measurement, *ACS Nano*, 2012, **6**, 4288–4297, DOI: **10.1021/nn300857d**.

157 K. Cao, S. Feng, Y. Han, L. Gao, T. Hue Ly, Z. Xu and Y. Lu, Elastic straining of free-standing monolayer graphene, *Nat. Commun.*, 2020, **11**, 284, DOI: **10.1038/s41467-019-14130-0**.

158 S. Zhang, Measuring the specific surface area of monolayer graphene oxide in water, *Mater. Lett.*, 2020, **261**, 127098.

159 J. B. Park and R. S. Lakes, *Biomaterials: an introduction*, Springer, New York, 3rd edn, 2007.

160 A. Aryaei, A. H. Jayatissa and A. C. Jayasuriya, Mechanical and biological properties of chitosan/carbon nanotube nanocomposite films: Chitosan/carbon nanotube nanocomposite films, *J. Biomed. Mater. Res., Part A*, 2014, **102**, 2704–2712, DOI: **10.1002/jbm.a.34942**.

161 P. E. Mikael, A. R. Amini, J. Basu, M. Josefina Arellano-Jimenez, C. T. Laurencin, M. M. Sanders, C. Barry Carter and S. P. Nukavarapu, Functionalized carbon nanotube reinforced scaffolds for bone regenerative engineering: Fabrication, *in vitro* and *in vivo* evaluation, *Biomed. Mater.*, 2014, **9**, 035001, DOI: **10.1088/1748-6041/9/3/035001**.

162 C. Gao, T. Liu, C. Shuai and S. Peng, Enhancement mechanisms of graphene in nano-58S bioactive glass scaffold: Mechanical and biological performance, *Sci. Rep.*, 2015, **4**, 4712, DOI: **10.1038/srep04712**.

163 R. Eivazzadeh-Keihan, A. Maleki, M. de la Guardia, M. S. Bani, K. K. Chenab, P. Pashazadeh-Panahi,

B. Baradaran, A. Mokhtarzadeh and M. R. Hamblin, Carbon based nanomaterials for tissue engineering of bone: Building new bone on small black scaffolds: A review, *J. Adv. Res.*, 2019, **18**, 185–201, DOI: **10.1016/j.jare.2019.03.011**.

164 B. L. Allen, P. D. Kichambare, P. Gou, I. I. Vlasova, A. A. Kapralov, N. Konduru, V. E. Kagan and A. Star, Biodegradation of single-walled carbon nanotubes through enzymatic catalysis, *Nano Lett.*, 2008, **8**, 3899–3903, DOI: **10.1021/nl802315h**.

165 E. Murray, B. C. Thompson, S. Sayyar and G. G. Wallace, Enzymatic degradation of graphene/polycaprolactone materials for tissue engineering, *Polym. Degrad. Stab.*, 2015, **111**, 71–77, DOI: **10.1016/j.polymdegradstab.2014.10.010**.

166 M. Yang, M. Zhang, H. Nakajima, M. Yudasaka, S. Iijima and T. Okazaki, Time-dependent degradation of carbon nanotubes correlates with decreased reactive oxygen species generation in macrophages, *Int. J. Nanomed.*, 2019, **14**, 2797–2807, DOI: **10.2147/IJN.S199187**.

167 V. E. Kagan, A. A. Kapralov, C. M. St. Croix, S. C. Watkins, E. R. Kisin, G. P. Kotchey, K. Balasubramanian, I. I. Vlasova, J. Yu, K. Kim, W. Seo, R. K. Mallampalli, A. Star and A. A. Shvedova, Lung macrophages "digest" carbon nanotubes using a superoxide/peroxynitrite oxidative pathway, *ACS Nano*, 2014, **8**, 5610–5621, DOI: **10.1021/nn406484b**.

168 R. Wang, R. Lohray, E. Chow, P. Gangupantula, L. Smith and R. Draper, Selective uptake of carboxylated multi-walled carbon nanotubes by class a type 1 scavenger receptors and impaired phagocytosis in alveolar macrophages, *Nanomaterials*, 2020, **10**, 2417, DOI: **10.3390/nano10122417**.

169 M. Sano, M. Izumiya, H. Haniu, K. Ueda, K. Konishi, H. Ishida, C. Kuroda, T. Uemura, K. Aoki, Y. Matsuda and N. Saito, Cellular responses of human lymphatic endothelial cells to carbon nanomaterials, *Nanomaterials*, 2020, **10**, 1374, DOI: **10.3390/nano10071374**.

170 N. R. Jacobsen, P. Møller, P. A. Clausen, A. T. Saber, C. Micheletti, K. A. Jensen, H. Wallin and U. Vogel, Biodistribution of carbon nanotubes in animal models, *Basic Clin. Pharmacol. Toxicol.*, 2017, **121**, 30–43, DOI: **10.1111/bcpt.12705**.

171 P. Ruenraroengsak, S. Chen, S. Hu, J. Melbourne, S. Sweeney, A. J. Thorley, J. N. Skepper, M. S.-P. Shaffer, T. D. Tetley and A. E. Porter, Translocation of functionalized multi-walled carbon nanotubes across human pulmonary alveolar epithelium: Dominant role of epithelial type 1 cells, *ACS Nano*, 2016, **10**, 5070–5085, DOI: **10.1021/acsnano.5b08218**.

172 M. Kucki, L. Diener, N. Bohmer, C. Hirsch, H. F. Krug, V. Palermo and P. Wick, Uptake of label-free graphene oxide by Caco-2 cells is dependent on the cell differentiation status, *J. Nanobiotechnol.*, 2017, **15**, 46, DOI: **10.1186/s12951-017-0280-7**.

173 H. Kafa, J. T.-W. Wang, N. Rubio, K. Venner, G. Anderson, E. Pach, B. Ballesteros, J. E. Preston, N. J. Abbott and K. T. Al-Jamal, The interaction of carbon nanotubes with an in vitro blood–brain barrier model and mouse brain in vivo, *Biomaterials*, 2015, **53**, 437–452, DOI: **10.1016/j.biomaterials.2015.02.083**.

174 Y. Chen, S. Pandit, S. Rahimi and I. Mijakovic, Interactions Between Graphene-Based Materials and Biological Surfaces: A Review of Underlying Molecular Mechanisms, *Adv. Mater. Interfaces*, 2021, **8**, 2101132, DOI: **10.1002/admi.202101132**.

175 F. Zhao, Y. Zhao, Y. Liu, X. Chang, C. Chen and Y. Zhao, Cellular uptake, intracellular trafficking, and cytotoxicity of nanomaterials, *Small*, 2011, **7**, 1322–1337, DOI: **10.1002/smll.201100001**.

176 B. Huang, Carbon nanotubes and their polymeric composites: the applications in tissue engineering, *Biomanufact. Rev.*, 2020, **5**, 3, DOI: **10.1007/s40898-020-00009-x**.

177 L. Lacerda, H. Ali-Boucetta, S. Kraszewski, M. Tarek, M. Prato, C. Ramseyer, K. Kostarelos and A. Bianco, How do functionalized carbon nanotubes land on, bind to and pierce through model and plasma membranes, *Nanoscale*, 2013, **5**, 10242, DOI: **10.1039/c3nr03184e**.

178 N. W. Shi Kam, T. C. Jessop, P. A. Wender and H. Dai, Nanotube molecular transporters: Internalization of carbon nanotube–protein conjugates into Mammalian cells, *J. Am. Chem. Soc.*, 2004, **126**, 6850–6851, DOI: **10.1021/ja0486059**.

179 X. Shi, Cell entry of one-dimensional nanomaterials occurs by tip recognition and rotation, *Nat. Nanotechnol.*, 2011, **6**, 6.

180 L. Lacerda, J. Russier, G. Pastorin, M. A. Herrero, E. Venturelli, H. Dumortier, K. T. Al-Jamal, M. Prato, K. Kostarelos and A. Bianco, Translocation mechanisms of chemically functionalised carbon nanotubes across plasma membranes, *Biomaterials*, 2012, **33**, 3334–3343, DOI: **10.1016/j.biomaterials.2012.01.024**.

181 Y. Sato, A. Yokoyama, Y. Nodasaka, T. Kohgo, K. Motomiya, H. Matsumoto, E. Nakazawa, T. Numata, M. Zhang, M. Yudasaka, H. Hara, R. Araki, O. Tsukamoto, H. Saito, T. Kamino, F. Watari and K. Tohji, Long-term biopersistence of tangled oxidized carbon nanotubes inside and outside macrophages in rat subcutaneous tissue, *Sci. Rep.*, 2013, **3**, 2516, DOI: **10.1038/srep02516**.

182 D. Kersting, S. Fasbender, R. Pilch, J. Kurth, A. Franken, M. Ludescher, J. Naskou, A. Hallenberger, C. von Gall, C. J. Mohr, R. Lukowski, K. Raba, S. Jaschinski, I. Esposito, J. C. Fischer, T. Fehm, D. Niederacher, H. Neubauer and T. Heinzel, From *in vitro* to *ex vivo*: Subcellular localization and uptake of graphene quantum dots into solid tumors, *Nanotechnology*, 2019, **30**, 395101, DOI: **10.1088/1361-6528/ab2cb4**.

183 B. Kang, S. Chang, Y. Dai, D. Yu and D. Chen, Cell response to carbon nanotubes: Size-dependent intracellular uptake mechanism and subcellular fate, *Small*, 2010, **6**, 2362–2366, DOI: **10.1002/smll.201001260**.

184 V. Neves, E. Heister, S. Costa, C. Tîlmaciu, E. Borowiak-Palen, C. E. Giusca, E. Flahaut, B. Soula, H. M. Coley, J. McFadden and S. R.-P. Silva, Uptake and release of

double-walled carbon nanotubes by Mammalian cells, *Adv. Funct. Mater.*, 2010, **20**, 3272–3279, DOI: 10.1002/adfm.201000994.

185 A. E. Porter, M. Gass, K. Muller, J. N. Skepper, P. A. Midgley and M. Welland, Direct imaging of single-walled carbon nanotubes in cells, *Nat. Nanotechnol.*, 2007, **2**, 713–717, DOI: 10.1038/nnano.2007.347.

186 M. Jennifer and W. Maciej, Nanoparticle technology as a double-edged sword: Cytotoxic, genotoxic and epigenetic effects on living cells, *J. Biomater. Nanobiotechnol.*, 2013, **04**, 53–63, DOI: 10.4236/jbnb.2013.41008.

187 Q. Mu, D. L. Broughton and B. Yan, Endosomal leakage and nuclear translocation of multiwalled carbon nanotubes: Developing a model for cell uptake, *Nano Lett.*, 2009, **9**, 4370–4375, DOI: 10.1021/nl902647x.

188 B. Rothen-Rutishauser, D. M. Brown, M. Piallier-Boyles, I. A. Kinloch, A. H. Windle, P. Gehr and V. Stone, Relating the physicochemical characteristics and dispersion of multiwalled carbon nanotubes in different suspension media to their oxidative reactivity *in vitro* and inflammation *in vivo*, *Nanotoxicology*, 2010, **4**, 331–342, DOI: 10.3109/17435390.2010.489161.

189 T. A. Tabish, C. J. Scotton, D. C.-J. Ferguson, L. Lin, A. van der Veen, S. Lowry, M. Ali, F. Jabeen, M. Ali, P. G. Winyard and S. Zhang, Biocompatibility and toxicity of graphene quantum dots for potential application in photodynamic therapy, *Nanomed.*, 2018, **13**, 1923–1937, DOI: 10.2217/nnm-2018-0018.

190 C. Ge, Y. Li, J.-J. Yin, Y. Liu, L. Wang, Y. Zhao and C. Chen, The contributions of metal impurities and tube structure to the toxicity of carbon nanotube materials, *NPG Asia Mater.*, 2012, **4**, e32, DOI: 10.1038/am.2012.60.

191 K. Pulskamp, S. Diabate and H. Krug, Carbon nanotubes show no sign of acute toxicity but induce intracellular reactive oxygen species in dependence on contaminants, *Toxicol. Lett.*, 2007, **168**, 58–74, DOI: 10.1016/j.toxlet.2006.11.001.

192 P.-X. Hou, C. Liu and H.-M. Cheng, Purification of carbon nanotubes, *Carbon*, 2008, **46**, 2003–2025, DOI: 10.1016/j.carbon.2008.09.009.

193 O. J. Yoon, I. Kim, I. Y. Sohn, T. T. Kieu and N.-E. Lee, Toxicity of graphene nanoflakes evaluated by cell-based electrochemical impedance biosensing: Toxicity of graphene nanoflakes, *J. Biomed. Mater. Res., Part A*, 2014, **102**, 2288–2294, DOI: 10.1002/jbm.a.34886.

194 V. Raffa, G. Ciofani, S. Nitodas, T. Karachalios, D. D'Alessandro, M. Masini and A. Cuschieri, Can the properties of carbon nanotubes influence their internalization by living cells?, *Carbon*, 2008, **46**, 1600–1610, DOI: 10.1016/j.carbon.2008.06.053.

195 S. H. Moolgavkar and R. C. Bro, Biopersistence, fiber length, and cancer risk assessment for inhaled fibers, *Inhal. Toxicol.*, 2001, **13**, 755–772, DOI: 10.1080/08958370121106.

196 M. Zhang, M. Yang, T. Morimoto, N. Tajima, K. Ichiraku, K. Fujita, S. Iijima, M. Yudasaka and T. Okazaki, Size-dependent cell uptake of carbon nanotubes by macrophages: A comparative and quantitative study, *Carbon*, 2018, **127**, 93–101, DOI: 10.1016/j.carbon.2017.10.085.

197 C. Wei, Z. Liu, F. Jiang, B. Zeng, M. Huang and D. Yu, Cellular behaviours of bone marrow-derived mesenchymal stem cells towards pristine graphene oxide nanosheets, *Cell Prolif*, 2017, **50**, e12367, DOI: 10.1111/cpr.12367.

198 J.-W. Kim, Y. Shin, J.-J. Lee, E.-B. Bae, Y.-C. Jeon, C.-M. Jeong, M.-J. Yun, S.-H. Lee, D.-W. Han and J.-B. Huh, The effect of reduced graphene oxide-coated biphasic calcium phosphate bone graft material on osteogenesis, *Int. J. Mol. Sci.*, 2017, **18**, 1725, DOI: 10.3390/ijms18081725.

199 M. van der Zande, R. Junker, X. F. Walboomers and J. A. Jansen, Carbon nanotubes in animal models: A systematic review on toxic potential, *Tissue Eng. Part B*, 2011, **17**, 57–69, DOI: 10.1089/ten.teb.2010.0472.

200 L. Newman, D. A. Jasim, E. Prestat, N. Lozano, I. de Lazaro, Y. Nam, B. M. Assas, J. Pennock, S. J. Haigh, C. Bussy and K. Kostarelos, Splenic capture and *in vivo* intracellular biodegradation of biological-grade graphene oxide sheets, *ACS Nano*, 2020, **14**, 10168–10186, DOI: 10.1021/acsnano.0c03438.

201 L. Lacerda, M. A. Herrero, K. Venner, A. Bianco, M. Prato and K. Kostarelos, Carbon-nanotube shape and individualization critical for renal excretion, *Small*, 2008, **4**, 1130–1132, DOI: 10.1002/smll.200800323.

202 D. A. Jasim, H. Boutin, M. Fairclough, C. Ménard-Moyon, C. Prenant, A. Bianco and K. Kostarelos, Thickness of functionalized graphene oxide sheets plays critical role in tissue accumulation and urinary excretion: A pilot PET/CT study, *Appl. Mater. Today*, 2016, **4**, 24–30, DOI: 10.1016/j.apmt.2016.04.003.

203 B. Sitharaman, X. Shi, X. F. Walboomers, H. Liao, V. Cuijpers, L. J. Wilson, A. G. Mikos and J. A. Jansen, In vivo biocompatibility of ultra-short single-walled carbon nanotube/biodegradable polymer nanocomposites for bone tissue engineering, *Bone*, 2008, **43**, 362–370, DOI: 10.1016/j.bone.2008.04.013.

204 N. Saito, H. Haniu, Y. Usui, K. Aoki, K. Hara, S. Takanashi, M. Shimizu, N. Narita, M. Okamoto, S. Kobayashi, H. Nomura, H. Kato, N. Nishimura, S. Taruta and M. Endo, Safe clinical use of carbon nanotubes as innovative biomaterials, *Chem. Rev.*, 2014, **114**, 6040–6079, DOI: 10.1021/cr400341h.

205 Y. Usui, K. Aoki, N. Narita, N. Murakami, I. Nakamura, K. Nakamura, N. Ishigaki, H. Yamazaki, H. Horiuchi, H. Kato, S. Taruta, Y. A. Kim, M. Endo and N. Saito, Carbon nanotubes with high bone-tissue compatibility and bone-formation acceleration effects, *Small*, 2008, **4**, 240–246, DOI: 10.1002/smll.200700670.

206 Y. C. Shin, J. H. Lee, O. S. Jin, S. H. Kang, S. W. Hong, B. Kim, J.-C. Park and D.-W. Han, Synergistic effects of reduced graphene oxide and hydroxyapatite on osteogenic differentiation of MC3T3-E1 preosteoblasts, *Carbon*, 2015, **95**, 1051–1060, DOI: 10.1016/j.carbon.2015.09.028.